Steric Effects of Alkyl Substituents at *N*-Donor Bidentate Amines Direct the Nuclearity, Bonding and Bridging Modes in Thiocyanato-Copper(II) Complexes

Franz A. Mautner [1,*], Roland C. Fischer [2], Ana Torvisco [2], Maher M. Henary [3], Andrew Milner [4], Hunter DeVillier [4], Tolga N. V. Karsili [4], Febee R. Louka [4] and Salah S. Massoud [4,*]

[1] Institut für Physikalische and Theoretische Chemie, Technische Universität Graz, A-8010 Graz, Austria; mautner@tugraz.at

[2] Institut für Anorganische Chemie, Technische Universität Graz, Stremayrgasse 9/V, A-8010 Graz, Austria; roland.fischer@tugraz.at, ana.torviscogomez@tugraz.at

[3] Department of Chemistry and Biochemistry, University of California, Los Angeles, CA 90095-1569, U.S.A. henary@chem.ucla.edu

[4] Department of Chemistry, University of Louisiana at Lafayette, P.O. Box 43700 Lafayette, LA 70504, U.S.A. tolga.karsili@louisiana.edu (T.K.); frl6631@louisiana.edu (F.R.L.); ssmassoud@louisiana.edu (S.S.M.); C00250551@louisiana.edu (A.M.); C00063128@louisiana.edu (H.De.V)

* Correspondence: ssmassoud@louisiana.edu, Tel. +01 337-482-5672

* Corresponding authors: E-mail: mautner@tugraz.at, Tel. ++43 316-4873-8234, fax: ++43 316-4873-8225 (F.A. Mautner); E-mail: ssmassoud@louisiana.edu, Tel. +01 337-482-5672, Fax: +01 337-482-5676 (S. S. Massoud).

Abstract: A series of Cu(II)-thiocyanato complexes derived from sterically hindered *N*-donors diamines were synthesized and characterized: *catena*-[Cu(Me$_3$en)(μ-NCS)(NCS)] (**1**), *catena*-[Cu(NEt$_2$Meen)(μ-NCS)(NCS)] (**2**), *catena*-[Cu(N,N,2,2-Me$_4$pn)(μ-NCS)(NCS)] (**3**), the dimeric: [Cu$_2$(N,N`-isp$_2$en)$_2$(μ-NCS)$_2$(NCS)$_2$] (**4**) and the monomeric complex [Cu(N,N`-*t*-Bu$_2$en)(NCS)$_2$] (**5**), where Me$_3$en = N,N,N`-Trimethylethylenediamine, NEt$_2$Meen = N,N-diethyl-N`-methylethylenediamine, N,N,2,2-Me$_4$pn = N,N,2,2-tetramethylpropylenediamine, N,N`-isp$_2$en = N,N`-diisopropylethylenediamine and N,N`-*t*-Bu$_2$en = N,N`-di(*tert*-butyl)ethylenediamine. The complexes were characterized by elemental microanalyse, IR and UV-Vis spectroscopy and single crystal X-ray crystallography. Density Functional Theory was used to evaluate the role of steric effects in compounds **4** and **5** and how this may affect the adaption of a specific geometry, NCS-bonding mode and the dimensionality of the resulting complex.

Keywords: Coordination Compounds; Coordination Polymers; Copper; Thiocyanate; Crystal Structure; DFT calculations

1. Introduction

Pseudohalide ligands are a class of compounds that are able to simultaneously bind two or more metal ions leading to the formation of di- or poly-nuclear metal complexes of different nuclearity, clusters and coordination polymers (CPs) of different dimensionality (1D, 2D, 3D) and topology [1-10]. However, the formation of these compounds depends largely on a number of factors which include which include electronic nature and oxidation state of metal ion, the nature of the coordinated ancillary co-ligand(s), its skeletal structure, and the steric hindrance imposed by the blocking coligand(s) surrounding the central metal ion [11,12]. Steric effects caused by the coordinating blocking ligands in metal complexes have been reported to produce a dramatic effect on the structural and magnetic behavior of pseudohalide complexes [1-11,13-16] but also in the biological catalytic reactions of the P-O bond in DNA and phosphodiester hydrolysis [17-20].

Thiocyanato complexes are considered as among the most studied systems in coordination chemistry due to the diverse bonding properties of NCS^- ion as an ambidentate and bridging ligand that can bind two or more metal ions simultaneously as well as its ability to propagate magnetic

Preprints (www.preprints.org) | NOT PEER-REVIEWED | Posted: 3 December 2018 doi:10.20944/preprints201812.0020.v1

Peer-reviewed version available at Crystals 2019, 9, 38; doi:10.3390/cryst9010038

interaction between the bridged paramagnetic metal ions. In general, several bonding modes were reported in bridging-thiocyanato-polynuclear and/or -polymeric metal complexes. These include the bonding modes $\mu_{1,3}$-NCS^- [1,5-7,10,21-31], $\mu_{1,1}$-NCS^- [32-34], $\mu_{3,3}$-NCS^- [35-37], $\mu_{1,1,3}$-NCS^- [38], $\mu_{1,3,3}$-NCS^-[39] and $\mu_{1,3,3,3}$-NCS^-[40]. In complexes where the coordinated thiocyanate ion is acting as a terminal ligand, then according to HSAB concept, soft Lewis acid metal ions prefer the soft Lewis *S*-site and hard metals prefer the soft site [41]. Interestingly, although the nitrogen in NCS^- is classified as a borderline Lewis base, most hard metals such as Fe^{2+}, Ni^{2+}, Cu^{2+}, Co^{2+}, and Zn^{2+} showed high preference to the *N*-site [42.43].

Herein, we report the synthesis and structural characterization of a series of Cu(II)-thiocyanato complexes which derived from sterically hindered *N*-donors diamines with different alkyl substituents as coligands: the coordination 1D-polymers: *catena*-[Cu(Me_3en)(μ-NCS)(NCS)] (**1**), *catena*-[Cu(NEt_2Meen)(μ-NCS)(NCS)] (**2**), *catena*-[Cu(N,N,2,2-Me_4pn)(μ-NCS)(NCS)] (**3**), the dimeric [Cu_2(N,N`-$isp_2$en)$_2$(μ-NCS)$_2$(NCS)$_2$] (**4**) and the monomeric complex [Cu(N,N`-*t*-Bu_2en)(NCS)$_2$] (**5**). This should allow us to evaluate the role of steric effect imposed by the coordinated amine coligands in adapting a specific NCS-bonding mode and the selected dimensionality. The structures of the ligands used in this study together with other related compounds are illustrated in Scheme1. The Density Functional theory computations were performed in an attempt to account for the observed geometrical and dimensionality of **4** and **5** complexes.

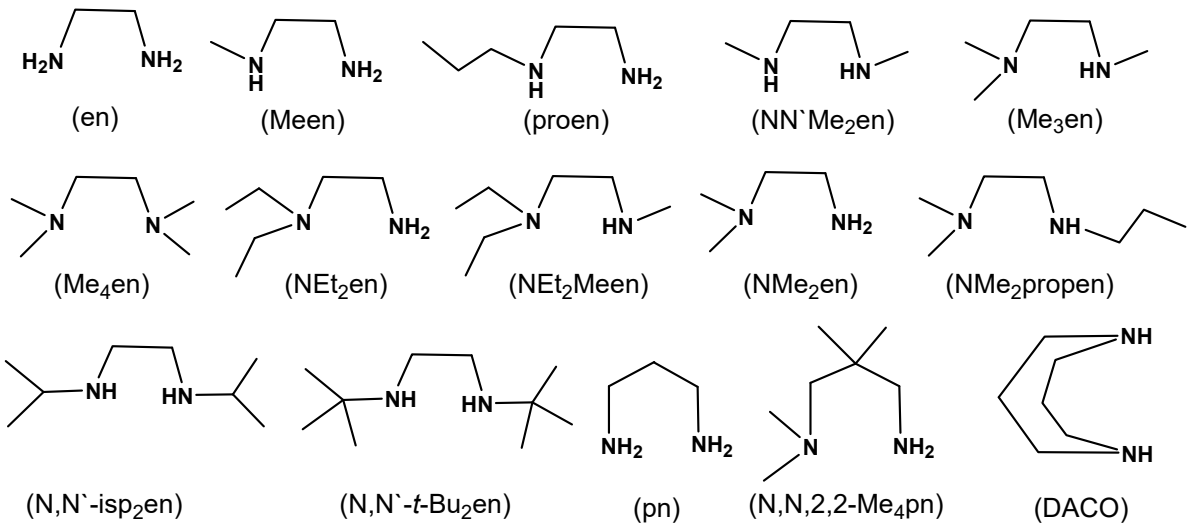

Scheme 1. Structures of the ligands used in this study together with other related compounds

2. Results and Discussion

2.1. Synthetic Aspects

The isolated complexes: *catena*-[Cu(Me$_3$en)(μ-NCS)(NCS)] (**1**), *catena*-[Cu(NEt$_2$Meen)(μ-NCS)(NCS)] (**2**), *catena*-[Cu(N,N,2,2-Me$_4$pn)(μ-NCS)(NCS)] (**3**), [Cu$_2$(N,N`-isp$_2$en)$_2$(μ-NCS)$_2$(NCS)$_2$] (**4**) and [Cu(N,N`-*t*-Bu$_2$en)(NCS)$_2$] (**5**) were synthesized in reasonably good yield (71-92%) and by the reaction of a methanolic solution containing equimolar amounts of Cu(NO$_3$)·3H$_2$O or Cu(ClO$_4$)$_2$·6H$_2$O and the corresponding diamine ligand with four equivalents of NH$_4$NCS solution dissolved in H$_2$O or MeOH. Crystals suitable for X-ray analysis were obtained from dilute solutions or by recrystallization from CH$_3$CN or anhydrous MeOH. The purity of the complexes was confirmed by elemental microanalyses (see experimental section). Molar conductivities, Λ_M measured in CH$_3$CN, are within the range of 7-12 Ω^{-1}cm^{2}mol^{-1} which reflect the non-electrolytic behavior of the complexes [44]. The complexes were also characterized by IR, UV-Vis and by single crystal X-ray crystallography. Probably, it is interesting to mention that although the μ-1,3- and μ-1,1-boding modes are common in bridging-azido-metal(II) complexes [8,9,11,12,14-16], the corresponding μ-1,1-bonding in the bridging-thiocyanato complexes is very rare [32-34] and in most cases alternating μ-1,3-bonding chains are observed [1-7,17,21-31].

2.2. IR and UV-VIS Spectra of the Complexes

The IR asymmetric stretching frequencies of the thiocyanato-Cu(II) complexes under investigation and their corresponding UV-Vis spectra in acetonitrile solution are collected in Table 1. It has been stated that the ν_{as}(C≡N) frequencies could be used as a criterion to differentiate between the terminally *N*-bonded thiocyanato anions which in most cases display a value below 2100 cm^{-1}, whereas in the corresponding *S*-bonded and/or μ-1,3-bridging thiocyanato anions, the stretching vibrations are observed above 2100 cm^{-1} [12,28-31,42,43,45]. The IR spectra of complexes **1**-**4** display very strong band over the 2095-2131 cm^{-1} region due to the asymmetric stretching vibration,ν_{as}(C≡N) of the bridged-thiocyanato ligands. In addition, the same series of complexes as well as **5** showed a strong to medium intensity band of the region 2059-3086 cm^{-1} which can be attributed to the *N*-bonded terminal thiocyanate ligand(s). This data are fully consistent with *N*-bonded thiocyanate in all complexes and μ-1,3-bridging thiocyanate in complexes **1**-**4** which was also confirmed by X-ray (section 2.3).

Inspection of the acetonitrile solutions of the UV-Vis spectral data of the complexes **1**-**4** shown in Table 1 reveals the common spectral feature as they display a broad absorption band in the 615-656 nm region. This feature is consistent with five-coordinate Cu(II) complexes with square pyramidal geometry (SP) which may be associated with a low-energy shoulder at $\lambda > 800$ nm [28-31,42,43,45-50]. The presence of a small intense band at 974 nm in complex **1** may reflect the increased distortion towards the trigonal bipyramidal geometry (TBP) [45]. Obviously, complex **4** does not belong to the observed geometry but instead it has one visible band at ~766 nm, resulting from d-d transition; $^2E \leftarrow {}^2T$ in tetrahedral environment [51]. The very strong intense band located at 469 nm can be assigned to ligand-metal charge transfer transition (L→M CT), whereas the 299 nm band is most likely attributed to electronic transition within the NCS^- ligand ($\pi \rightarrow \pi^*$). The geometrical finding around the Cu(II) ion in acetonitrile solution was retained in the solid state as it supported with the X-ray structural data.

Table 1. The IR asymmetric stretching frequency of the coordinated thiocyanato groups and UV-Vis spectra of the complexes **1**-**5** in CH_3CN solution.

Complex	$\nu_{as}(C\equiv N)$ (cm^{-1})	λ_{max}, nm (ε, $M^{-1}cm^{-1}$)
catena-[Cu(Me$_3$en)(μ-NCS)(NCS)] (**1**)	2131 (vs), 2086 (vs)	615 (153), 974 (59)
catena-[Cu(NEt$_2$Meen)(μ-NCS)(NCS)] (**2**)	2095 (vs), 2025 (m)	655 (159)
catena-[Cu(N,N,2,2-Me$_4$pn)(μ-NCS)(NCS)] (**3**)	2099 (vs), 2068 (vs)	~656 (136)
[Cu$_2$(N,N`-isp$_2$en)$_2$(μ-NCS)$_2$(NCS)$_2$] (**4**)	2128 (s), 2073 (vs)	~655 (120)
[Cu(N,N`-*t*-Bu$_2$en)(NCS)$_2$] (**5**)	2059 (vs)	~766 (266), 469 (2160), 299 (3090)

2.3. Description of the Structures

2.3.1. *catena*-[Cu(Me$_3$en)(μ-NCS)(NCS)] (**1**), *catena*-[Cu(NEt$_2$Meen)(μ-NCS)(NCS)] (**2**) and *catena*-[Cu(N,N,2,2-Me$_4$pn)(μ-NCS)(NCS)] (**3**)

Perspective views together with the atom numbering scheme for the polymeric complexes **1** – **3** are presented in Figures 1 - 3, respectively, and selected bond parameters are given in Tables S1 – S3. The copper centers are linked by single $\mu_{1,3}$-thiocyanato bridges to form polymeric chains of polyhedra (1D). Each metal center is *penta*-coordinated by two *N*-donor atoms of the amine ligands, two *N*-atoms of terminal and bridging NCS^- anions and *S*-atom of bridging NCS^- anion. Their CuN_4S

chromophores may be described as distorted as SP geometry with τ values of 0.01, 0.42 and 0.21, for **1** – **3**, respectively (τ values of 0 and 1 refer to ideal SP and TBP geometries, respectively) [52]. The basal Cu-N bond distances are in the range from 1.9487(13) to 2.106(7) Å. The apical positions are occupied by the S-atoms of the bridging NCS^- groups [Cu-S from 2.6421(11) to 2.8910(16)]. The NCS^- groups have the following bond parameters: Cu-N-C: from 155.8(8) to 168.6(4)°; N-C-S: from 178.6(5) to 179.8(4)°; N-C: from 1.150(6) to 1.167(6) Å; C-S: from 1.633(4) to 1.642(4) Å. The intra-chain Cu···Cu' distances are 5.4245(11), 5.7755(9) and 5.7679(15) Å, for **1** – **3**, respectively. The shortest inter-chain metal-metal separations are 6.7646(16), 6.8602(10) and 6.9132(16) Å, for **1** – **3**, respectively. The bridging N-C-S groups form the following torsion angles: Cu-N-C-S: 23.2°, 23.2°, 23.2°; the Cu'-S-C-N: -139.4, -139.4 and 87.9°, for **1** – **3**, respectively. Hydrogen bonds of type N-H···S are formed between N atoms of amine ligand to S atom of neighboring Cu-polyhedra (Figures S1 – S3) [N(1)···S(1#) ((#) 1/2+x, 1/2-y, -z) = 3.446(4) Å, N(1)-H(1)···S(1#) = 147° for (**1**); N(1)···S(3#) ((#) x, 1/2-y, 1/2-z) = 3.519(3) Å, N(1)-H(90)···S(3#) = 158° for (**2**); N(3)···S(1#) ((#) x, 1/2-y, -1/2+z) = 3.573(7) Å, N(3)-H(3A)···S(1#) = 166° and N(3)···S(1+) ((+) 2-x, -1/2+y, -1/2-z) = 3.492(7) Å, N(3)-H(3B)···S(1+) = 158° for (**3**)] to form a supramolecular 2D system in case of **3**.

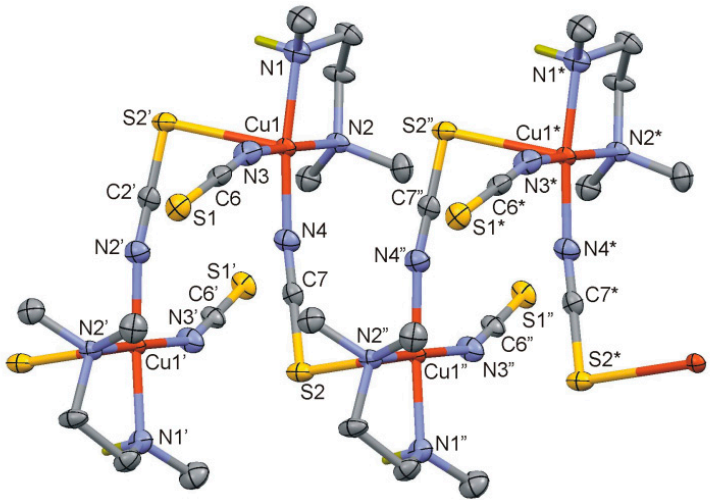

Figure 1. Perspective view of a section of the polymeric chain of **1**. Symmetry codes: (') 3/2-x,1-y,1/2+z; (") 3/2-x,1-y,-1/2+z; (*) x,y,-1+z.

Preprints (www.preprints.org) | NOT PEER-REVIEWED | Posted: 3 December 2018 doi:10.20944/preprints201812.0020.v1

Peer-reviewed version available at Crystals 2019, 9, 38; doi:10.3390/cryst9010038

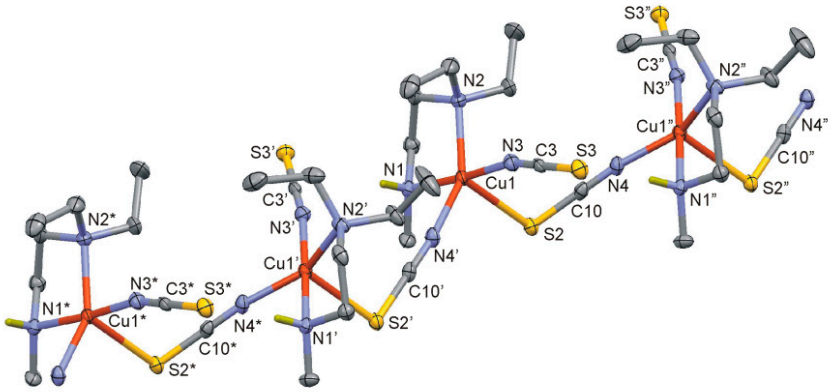

Figure 2. Perspective view of a section of the polymeric chain of **2**. Symmetry codes: (‘) x,1/2-y,-1/2+z; (“) x,1/2-y,1/2+z; (*) x,y,-1+z.

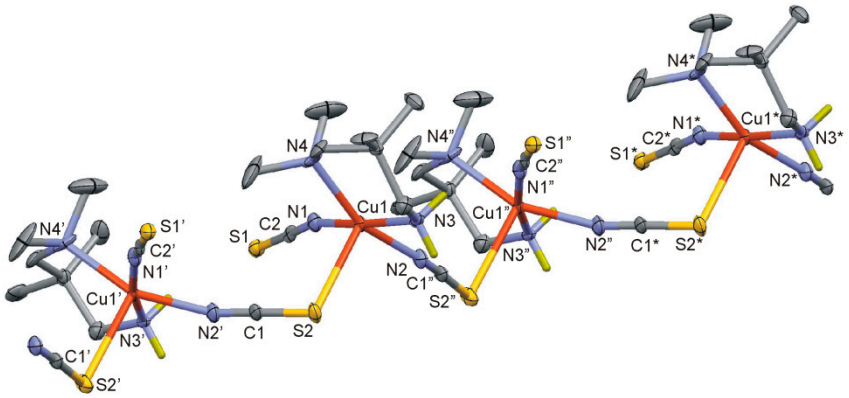

Figure 3. Perspective view of a section of the polymeric chain of **3**. Symmetry codes: (‘) x,1/2-y,1/2+z; (“) x,1/2-y,-1/2+z; (*) x,y,-1+z.

2.3.2. $[Cu_2(N,N`\text{-}isp_2en)_2(\mu\text{-}NCS)_2(NCS)_2]$ (**4**)

Complex **4** consists of centrosymmetric dimeric $[Cu_2(N,N'\text{-}isp_2en)_2(\mu\text{-}NCS)_2(NCS)_2]$ units (Figure 4). Each Cu center is *penta*-coordinated by two N-atoms of N,N’-isp_2en ligand, two N-atoms of terminal and bridging NCS^- anions and S-atom of bridging NCS^- anion. The CuN_4S chromophore may be described as distorted polyhedron with intermediate geometry between square pyramidal (SP) and trigonal bipyramidal (TBP) with a τ value of 0.50. The apical site is occupied by the S(1’) atom [Cu(1)-S(1’) = 2.9037(6) Å]. The basal Cu-N bonds vary from 1.9487(13) to 2.0388(12) Å.

The NCS^- groups have the following bond parameters: Cu-N-C: 179.19(13) and 163.99(11)°; N-C-S: 179.19(13) and 178.89(13)°; N-C: 1.1562(19) and 1.1612(19) Å; C-S: 1.6420(14) and 1.6306(15) Å. The centrosymmetric dimeric units are built by $\mu_{1,3}$-thiocyanato double bridges. Their eight-membered $Cu(NCS)_2Cu$ rings are almost planar ["chair angle" θ which is defined as acute angle between plane of the di-$\mu_{1,3}$-thiocyanato bridges and the Cu/N(1)/S(1) plane is 2.5°]. The Cu(1)···Cu(1') distance within the $Cu(NCS)_2Cu$ ring is 5.8794(8) Å, and the inter-dimer separation is 6.6979(9) Å. The Cu-N···S-Cu' torsion angle is 23.2°, the Cu-N-C-S torsion angles are -139.4 and 87.9°. Hydrogen bonds of type N-H···S are formed between N(3) atoms of N,N'- isp_2en ligand to S(1) atom of neighboring Cu-polyhedra (Figure S4) [N(3)···S(1#) ((#) x,1/2-y,1/2+z) = 3.4703(13) Å, N(3)-H(31)···S(1#) = 157°].

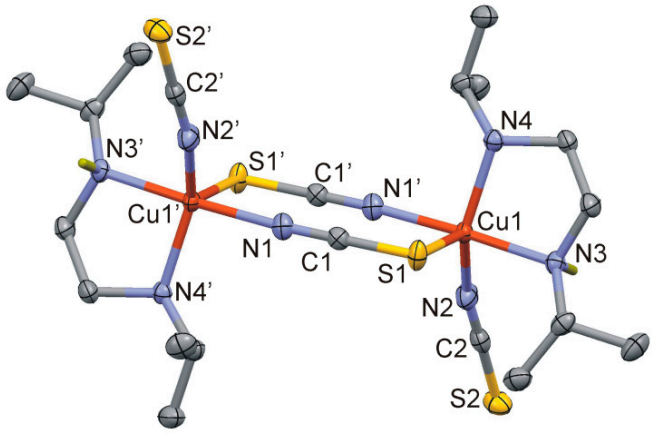

Figure 4. Perspective view of the dimeric complex **4**. Symmetry code: (') 2-x,-y,-z.

2.3.3. $[Cu(N,N`-t-Bu_2en)(NCS)_2]$ (**5**)

The title complex **5** consists of monomeric neutral $[Cu(N,N'-t-Bu_2en)(NCS)_2]$ units where the Cu centers are tetrahedrally coordinated by four nitrogen donor atoms: two belong to the N,N'-*t*-Bu_2en ligand and two belong to *N*-terminal thiocyanato anions (Figure 5). The Cu-N bond distances are in the range from 1.9299(17) to 2.0108(16) Å. The distorted coordination tetrahedra form N-Cu-N bond angles in the range from 97.03(7) to 140.14(7)°. The terminal thiocyanato anions have the following bond parameters: N-C: 1.156(3) and 1.165(3) Å; C-S: 1.637(2) and 1.618(2) Å; N-C-S: 179.8(18) and 179.6(2)°; Cu-N-C: 161.74(16) and 160.42(17)°. The shortest Cu···Cu separation is 6.4592(9) Å. Hydrogen bonds of type N-H···S are formed between N(3) and N(4) atoms of N,N'-*t*-Bu_2en ligand to S(1) atoms of neighboring Cu-polyhedra to generate a supramolecular 2D system

Preprints (www.preprints.org) | NOT PEER-REVIEWED | Posted: 3 December 2018 doi:10.20944/preprints201812.0020.v1

Peer-reviewed version available at Crystals 2019, 9, 38; doi:10.3390/cryst9010038

oriented along the *b*- and *c*-axis of the unit cell (Figure S5) [N(3)···S(1#) ((#) 2-x,-y,-z) = 3.3917(17) Å, N(3)-H(31)···S(1#) = 173°; N(4)···S(1+) ((+) x,1/2-y,-1/2+z) = 3.4694(17) Å, N(4)-H(41) ···S(1+) = 171°].

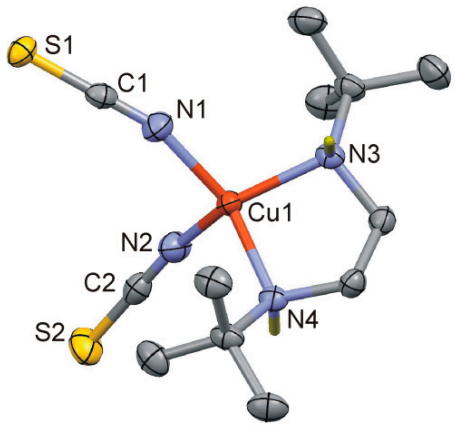

Figure 5. Molecular plot of **5**.

We think it would be interesting to compare our structural results of compounds **1**-**5** with the literature data of Cu(II)-thiocyanato complexes which derived from related bidentate amines and these compounds together with ours are collected in Table 2. Inspection of this data may show some general trends about the coordination behavior of these complexes. The thiocyanato complexes which are constructed from ethylenediamine (en) [53-57], mono-*N*-alkyl ethylenediamine (Me-en, propen) [61,62], less hindered di(*N,N*`-alkyl)-ethylenediamine (N,N`-Me$_2$en) [60] and DACO [63] resulted in the formation of mono-nuclear Cu(II)-bis(diamine) complexes with or without *N*-NCS-coordination. With very bulky di(*N,N*`-alkyl)-ethylenediamine; N,N`-*t*-Bu$_2$en, only mono-nuclear Cu(II)-(diamine), [Cu(N,N`-*t*-Bu$_2$en)(NCS)$_2$] (**5**) was formed without *N*-NCS-coordination. However, when one of the methyl groups in each of the *tert*-butyl moieties in N,N`-*t*-Bu$_2$en was replaced by hydrogen to moderate and relief the steric environment (N,N`-isp$_2$en), the dinuclear bridged-NCS complex [Cu$_2$(N,N`-isp$_2$en)$_2$(μ_2-NCS)$_2$(NCS)$_2$] (**4**) was isolated. On the other hand, the thiocyanato complexes which were constructed from N,N-dialkyl, N,N,N`-trialkyl- and/or tetra-N,N,N`,N`-tetraalky-diamine ligands afforeded the five-coordinate 1D-polymeric chains where the Cu(II)-(diamine) moieties are $\mu_{N,S}$-NCS bridged and the coordination geometry is achieved by another *N*-NCS group [64-67] as this was the case observed in the **1**-**3** complexes under investigation.

Table 2. Some structural details of Cu(II)-thiocyanate complexes derived from some *N*-alkyl bidentate amine ligands.[a)]

Compound	C.N.; Nuc.[b)]	NCS-bonding	Refcode [Ref]
$[Cu(en)_2]Br(NCS)$	4; mono	non-coord.	BITJIX [53]
$[Cu(en)_2](NCS)(ClO_4)$	4; mono	non-coord.	ENCUTP [54]
$[Cu(en)_2](NCS)_2$	4; mono	non-coord.	EDCOPT [55]
$[Cu(en)_2](NCS)(BF_4)$	4; mono	non-coord.	GASRUN [56]
$[Cu(en)_2](NCS)_2$	4; mono	non-coord.	TCENCU [57]
$[Cu(en)(NCS)_2(H_2O)]$	5; mono	*N*-NCS	HIQGUJ [58]
$[Cu(Me\text{-}en)_2(NCS)](NCS)$	5; mono	*N*-NCS, non-coord.	MEENCU [59]
$[Cu(N,N`\text{-}Me_2en)_2](NCS)_2$	4; mono	non-coord.	MENCUT [60]
$[Cu(propen)_2](NCS)_2$	4; mono	non-coord.	APRCUT [61]
$[Cu(propen)_2(NCS)]ClO_4$	5; mono	*N*-NCS	DAPICU [62]
$[Cu(DACO)_2(NCS)](NCS)(H_2O)$	5; mono	*N*-NCS, non-coord.	FEKHAF [63]
$[Cu(N,N`\text{-}t\text{-}Bu_2en)(NCS)_2]$ (**5**)	4; mono	*N*-NCS	This work
$[Cu_2(N,N`\text{-}isp_2en)_2(\mu_2\text{-}NCS)_2(NCS)_2]$ (**4**)	5, dimer	di-$\mu_{N,S}$, *N*-NCS	This work
catena-$[Cu(NEt_2en)(\mu\text{-}NCS)(NCS)]$	5, 1D	$\mu_{N,S}$, *N*-NCS	XIBXAI [64]
catena-$[Cu(Me_4en)(\mu\text{-}NCS)(NCS)]$	5; 1D	$\mu_{N,S}$, *N*-NCS	DUBNIZ [65]
catena-$[Cu(Me_3en)(\mu\text{-}NCS)(NCS)]$ (**1**)	5, 1D	$\mu_{N,S}$, *N*-NCS	This work
catena-$[Cu(NEt_2Meen)(\mu\text{-}NCS)(NCS)]$ (**2**)	5, 1D	$\mu_{N,S}$, *N*-NCS	This work
catena-$[Cu(NMe_2propen)\ (\mu\text{-}NCS)(NCS)]$	5; 1D	$\mu_{N,S}$, *N*-NCS	SEZFAF [66]
catena-$[Cu(N,N,2,2\text{-}Me_4pn)(\mu\text{-}NCS)(NCS)]$ (**3**)	5, 1D	$\mu_{N,S}$, *N*-NCS	This work
catena-$[Cu(DACO)(\mu\text{-}NCS)(NCS)]$	5; 1D	$\mu_{N,S}$, *N*-NCS	FODQOF [67]

[a)] Structures of the ligands and their abbreviations are shown in shown in Scheme 1.
[b)] C.N. = coordination number of Cu(II) and Nuc = nuclearity

2.4. The DFT Computational Results

DFT was used in order to garner insights into the aggregation properties of the various Cu complexes. In particular, we are interested in the intrinsic reasons for the ligand specific variations in adapting certain mono- or polynuclear chain size. Figure 6 shows the geometries and energetics associated with various oligomeric arrangements of **5** and **4**. Figure 6(a) shows the ground state minimum energy geometry of Cu(I), Cu(II) and Cu(III) oxidation states of monomeric **5**; The N,N'-*t*-Bu_2en ligand tends to form a mononuclear tetrahedral arrangement around the metal center which is in good agreement with the X-ray crystal structure results. The Cu(I) is the lowest energy charge of **5** is -1, which can be understood by considering that the entire complex is closed-shell when Cu is in the +1 oxidation state. Attempts were made to dimerizing **5** with overall charges of neutral, +1 and -1. Upon optimization, the neutral complex associates and forms a stable dimer, the +1 and -1

Preprints (www.preprints.org) | NOT PEER-REVIEWED | Posted: 3 December 2018 doi:10.20944/preprints201812.0020.v1

Peer-reviewed version available at Crystals 2019, 9, 38; doi:10.3390/cryst9010038

charged **5** dimers dissociate and form a monomer pair at an asymptotic separation. The neutral complex forms a stable dimer but it is at a higher energy state when compared the -1 complex of **5**. Thus, the Cu(I) complex **5** is the lowest energy oxidation state of the metal-center and yields a complex with an overall charge of -1; The -1 charge of **5** leads to prompt dissociation of a dimer upon geometry optimization – forming two monomers.

Analogous computations on **4** also returned Cu(I) as the lowest energy oxidation state of the metal-center. Attempts to dimerizing **4** were successful for the lowest energy triplet state of Cu(II) (henceforth ^{3}Cu(II)) oxidation state and, unlike **5**, did not dissociated to form two monomers upon optimization. The dimer form of triplet-Cu(II) of **4** is lower that the monomer forms by ~16 kcal/ mol. All other oxidation states of Cu of **4** failed to converge to a dimer and yielded two monomers. However, further attempts to trimerize **4** were unsuccessful and yielded a dimer + monomer at an infinite separation upon optimization. This observation is again in line with the observed dimeric crystal structure of **4**.

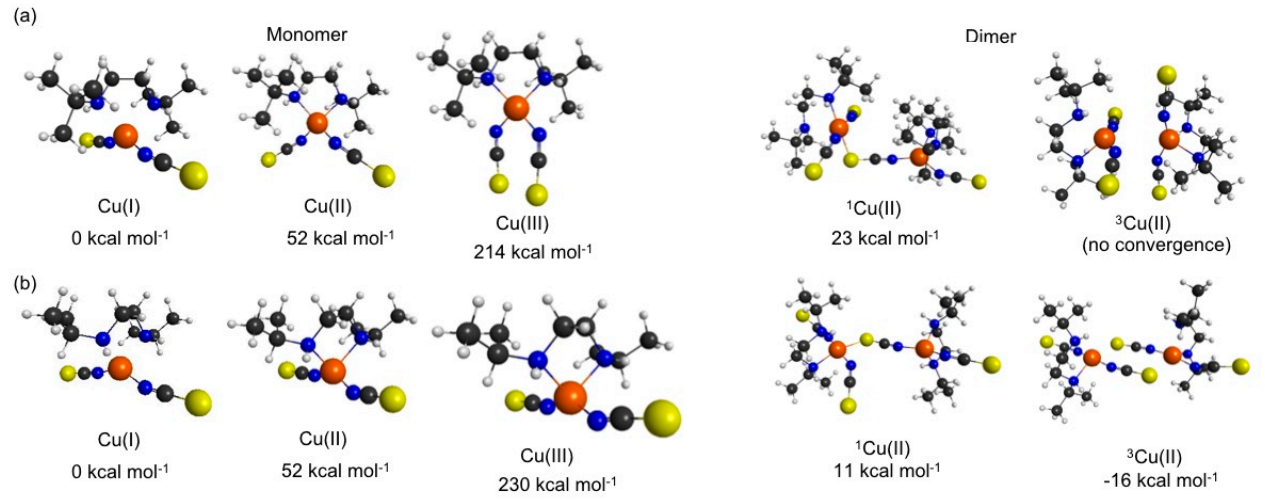

Figure 6. Geometries associated with the ground state minima of (a) **5** and (b) **4**. The Dimer geometries are relative to the energy of the Cu(II) + Cu(II) monomer asymptote at infinite separation.

In comparing **5** with **4**, we postulate that the bulky *tert*-butyl moiety in **5** shows an enhanced steric hindrance, thus inhibiting its ability to sustain a polymeric structure. The loss of two methyl groups in **5** leads to some reduction in such steric hindrance. As a result, **4** is able to sustain a

dimeric crystal structure but unable to maintain a larger oligomeric arrangement since $(en)_2$ remains a bulky group that introduced steric hindrances. With the available resources and large molecular sizes, complexes **1**, **2** and **3** produced computationally challenging. However, using the available computational data for **5** and **4** we are able to postulate that similar steric arguments would hold in the cases of **1** - **3** since the bulky *N*-alkyl substituents at the ethylenediamine coligand becomes progressively less favorable across this series.

3. Experimental Section

3.1. Materials and Physical Measurements

N,N,N`-Trimethylethylenediamine ($Me_3en$), N,N-diethyl-N`-methylethylenediamine (Et_2Meen), N,N,2,2-tetramethylpropylenediamine (N,N,2,2-Me_4pn), N,N`-diisopropylethylene-diamine (N,N`-isp_2en) and N,N`-di(*tert*-butyl)ethylenediamine (N,N`-*t*-Bu_2en) were purchased from TCI-America. All other chemicals were commercially available and used without further purification. Infrared spectra were recorded on a Cary 630 (FT IR-ATR) spectrometer. Electronic spectra were recorded using an Agilent 8453 HP diode array UV-Vis spectrophotometer. The conductivity measurements were performed using a Mettler Toledo Seven Easy conductivity meter, calibrated by the aid of a 1413 µS/cm conductivity standard. Elemental analyses were performed by the Atlantic Microlaboratory, Norcross, Georgia U.S.A.

3.2. Syntheses of the complexes

Catena-[Cu(Me_3en)(µ-NCS)(NCS)] (**1**). A mixture of $Cu(ClO_4)_2{\cdot}6H_2O$ (0.186 g, 0.5 mmol), N,N,N`-trimethylethylenediamine (Me_3en) (0.051 g, 0.50 mmol) and NH_4NCS (0.152 g, 2.0 mmol) was dissolved in MeOH (20 mL) and the resulting dark green solution was heated for 5 min, filtered while hot and allowed to stand at room temperature. The precipitate obtained after two hrs was collected and crystallized from CH_3CN to afford navy blue single crystals. These were collected by filtration, washed with propan-2-ol, Et_2O and air dried (yield: 0.105 g, 74%). Anal. Calcd for $C_7H_{14}CuN_4S_2$ (MM = 281.89 g/mol): C, 29.83, H, 5.01, N, 19.88%. Found: C, 29.92, H, 4.86, N, 19.92%. Selected IR bands (ATR-IR, cm^{-1}): 3178 (w) (N-H stretching), 2921 (w) (aliphatic C-H stretching), 2131 (vs), 2086 (vs) (C≡N stretching of NCS^-). UV-Vis spectrum {λ_{max}, nm (ε, $M^{-1}cm^{-1}$)} in CH_3CN: 615 (153), 974 (59). Λ_M (CH_3CN) = 8 $\Omega^{-1}cm^2mol^{-1}$.

Catena-[Cu(Et$_2$Meen)(μ-NCS)(NCS)] (**2**). To a mixture containing Cu(NO$_3$)$_2$·3H$_2$O (0.241g, 1.0 mmol), N,N-diethyl-N`-methylethylenediamine (Et$_2$Meen) (0.130 g, 1.0 mmol) dissolved in MeOH (25 mL), an aqueous solution of NH$_4$NCS (0.152 g, 2.0 mmol dissolved in 5 mL H$_2$O) was added dropwise and the reaction mixture was heated for 5 min, filtered through celite and then allowed to crystallize at room temperature. The green precipitate which separated after one day was collected and recrystallized from anhydrous MeOH and the resulting long needle crystals were collected by filtration, washed with propan-2-ol, Et$_2$O and air dried (yield: 0.227 g, 73%). Anal. Calcd for C$_9$H$_{18}$CuN$_4$S$_2$ (MM = 309.94 g/mol): C, 34.88; H, 5.85; N, 18.08%. Found: C, 35.02, H, 5.97, N, 17.89%. Selected IR bands (ATR-IR, cm^{-1}): 3168 (w) (N-H stretching), 2974 (w), 2933 (vw), 2878 (vw) (aliphatic C-H stretching), 2095 (vs) (C≡N stretching of NCS$^-$). UV-Vis spectrum {λ_{max}, nm (ε, M^{-1}cm^{-1})} in CH$_3$CN: 655 (159). Λ_M (CH$_3$CN) = 11 Ω^{-1}cm^{2}mol^{-1}.

Catena-[Cu(N,N,2,2-Me$_4$pn)(μ-NCS)(NCS)] (**3**). This complex was isolated as green single crystals and prepared using a similar procedure to that described for **2**, except N,N,2,2-tetramethylpropylenediamine was used instead of Et$_2$Meen (yield: 92%). Anal. Calcd for C$_9$H$_{18}$CuN$_4$S$_2$ (MM = 309.94 g/mol): C, 34.88; H, 5.85; N, 18.08%. Found: C, 34.67; H, 5.55; N, 18.30%. Selected IR bands (ATR-IR, cm^{-1}): 3291 (w), 3225 (N-H stretching), 2995 (vw), 2965 (w), 2886 (vw), 2842 (vw) (aliphatic C-H stretching), 2099 (vs), 2068 (vs) (C≡N stretching of NCS$^-$). UV-Vis spectrum {λ_{max}, nm (ε, M^{-1}cm^{-1})} in CH$_3$CN: ~656 (136). Λ_M (CH$_3$CN) = 12 Ω^{-1}cm^{2}mol^{-1}.

*[Cu$_2$(N,N`-isp$_2$en)$_2$(μ$_2$-NCS)$_2$(NCS)$_2$]* (**4**). Green single crystals of X-ray quality were obtained from a methanolic solution using a procedure similar to that described for **2**, with N,N`-diisopropylethylenediamine (N,N`-isp$_2$en) was used instead of Et$_2$Meen (yield: 79%). Anal. Calcd for C$_{20}$H$_{40}$Cu$_2$N$_8$ S$_4$ (MM = 647.94 g/mol): C, 37.08; H, 6.22; N, 17.29%. Found: C, 36.80; H, 6.06; N, 17.25%. Selected IR bands (ATR-IR, cm^{-1}): 3213 (w), 3158 (w) (N-H stretching), 2975 (w), 2964 (vw), 2925 (vw), 2876 (vw) (aliphatic C-H stretching), 2128 (s), 2073 (vs) (C≡N stretching of NCS$^-$). UV-Vis spectrum {λ_{max}, nm (ε, M^{-1}cm^{-1})} in CH$_3$CN: ~655 (120). Λ_M (CH$_3$CN) = 12 Ω^{-1}cm^{2}mol^{-1}.

*[Cu(N,N`-t-Bu$_2$en)(NCS)$_2$]* (**5**). Green single crystals of X-ray quality were obtained from a methanolic solution using a procedure similar to that described for **2**, with N,N`-di(*tert*-butyl)ethylenediamine (N,N`-*t*-Bu$_2$en) was used instead of Et$_2$Meen (yield: 71%). Anal. Calcd for C$_{12}$H$_{24}$CuN$_4$S$_2$ (MM = 352.02 g/mol): C, 40.94; H, 6.87; N, 15.92%. Found: C, 41.08; H, 6.72; N, 16.21%. %. Selected IR bands (ATR-IR, cm^{-1}): 3242 (m) (N-H stretching), 2972 (w), 2859 (vw)

(aliphatic C-H stretching), 2059 (vs) (C≡N stretching of NCS^-). UV-Vis spectrum {λ_{max}, nm (ε, $M^{-1}cm^{-1}$)} in CH_3CN: ~766 (266), 469 (2160), 299 (3090). Λ_M (CH_3CN) = 7 $\Omega^{-1}cm^2mol^{-1}$.

3.3. X-ray crystal structure analysis and refinement

The X-ray single-crystal data of compounds **1-5** were collected on a Bruker-AXS APEX II CCD diffractometer at 100(2) K. The crystallographic data, conditions retained for the intensity data collection and some features of the structure refinements are listed in Tables 3 and 4. The intensities were collected with Mo-Kα radiation (λ= 0.71073 Å). Data processing, Lorentz-polarization and absorption corrections were performed using SAINT, APEX and the SADABS computer programs [68]. The structures were solved by direct methods and refined by full-matrix least-squares methods on F^2, using the SHELXTL program package [69]. All non-hydrogen atoms were refined anisotropically. The hydrogen atoms were located from difference Fourier maps, assigned with isotropic displacement factors and included in the final refinement cycles by use of geometrical constraints. Molecular plots were performed with the MERCURY program [70].

CCDC 1878247-1878251 contain the supplementary crystallographic data for complexes **1** - **5**, respectively. These data can be obtained free of charge from The Cambridge Crystallographic Data Centre via www.ccdc.cam.ac.uk/data_request/cif.

Table 3. Crystallographic data and processing parameters for **1** – **3**.

Compound	**1**	**2**	**3**
Empirical formula	$C_7H_{14}CuN_4S_2$	$C_9H_{18}CuN_4S_2$	$C_9H_{18}CuN_4S_2$
Formula mass	281.89	309.94	309.94
System	Orthorhombic	Monoclinic	Monoclinic
Space group	$P2_12_12_1$	P $2_1/c$	P $2_1/c$
a (Å)	10.9708(6)	12.5637(13)	10.2410(11)
b (Å)	15.6954(9)	10.6338(11)	13.1290(14)
c (Å)	6.7646(4)	10.9288(12)	10.2040(11)
α (°)	90	90	90
β (°)	90	105.709(13)	92.308(19)
γ (°)	90	90	90
V ($Å^3$)	1164.80(12)	1405.6(3)	1370.9(3)
Z	4	4	4

T (K)	100(2)	100(2)	100(2)
μ (mm^{-1})	2.202	1.832	1.878
D_{calc} (Mg/m^3)	1.607	1.465	1.502
Crystal size (mm)	0.09 × 0.07 × 0.05	0.40 × 0.08 × 0.04	0.22 × 0.10 × 0.08
θ max (°)	33.207	26.332	25.25
Data collected	48125	10871	9720
Unique refl. / R_{int}	4443 / 0.1330	2860 / 0.0587	2469 / 0.0908
Parameters	142	151	149
Goodness-of-Fit on F^2	1.049	1.065	1.287
R1 / wR2 (all data)	0.0502 / 0.1157	0.0497 / 0.1089	0.0981 / 0.2129
Residual extrema ($e/Å^3$)	1.61 / -0.77	0.73 / -0.50	1.62 / -1.00

Table 4. Crystallographic data and processing parameters for **4** and **5**.

Compound	**4**	**5**
Empirical formula	$C_{20}H_{40}Cu_2N_8S_4$	$C_{12}H_{24}CuN_4S_2$
Formula mass	647.94	352.02
System	Monoclinic	Monoclinic
Space group	P $2_1/c$	P $2_1/c$
a (Å)	8.3074(10)	9.0079(11)
b (Å)	12.4648(13)	13.2386(13)
c (Å)	14.4011(15)	14.7134(14)
α (°)	90	90
β (°)	106.187(3)	103.156(3)
γ (°)	90	90
V ($Å^3$)	1432.1(3)	1432.1(3)
Z	2	4
T (K)	100(2)	100(2)
μ (mm^{-1})	1.802	1.516
D_{calc} (Mg/m^3)	1.503	1.368
Crystal size (mm)	0.30 × 0.18 × 0.13	0.33 × 0.22 × 0.15
θ max (°)	26.310	26.365
Data collected	11053	13358
Unique refl. / R_{int}	2894 / 0.0252	3646 / 0.0327
Parameters	164	184
Goodness-of-Fit on F^2	1.057	1.063
R1 / wR2 (all data)	0.0203 / 0.0537	0.0295 / 0.0756
Residual extrema ($e/Å^3$)	0.34 / -0.43	0.41 / -0.21

3.4. The Computational Methodology

The ground state minimum energy geometry of the various structures was optimized with density functional theory (DFT), using the Becke-3 parameter-Lee-Yang-Parr (B3LYP) functional [71] and the 6-31G(d) Pople basis set [72]. The increasing size and molecular complexity of the oligomeric metal complexes precluded the use of higher levels of theory. The B3LYP/6-31G(d) level is therefore an adequate compromise between accuracy and computational expense and allows for a qualitative comparison between polymers of varying size. The individual Cu-complexes may associate to form oligomers of varying chain length. Association energies were calculated by optimizing a given polymer and their associated monomers and smaller oligomers that make up the polymers. Computations were performed on both Cu(I) and Cu(III) oxidation states in order to determining the dominant oxidation state in a given oligomer. The Gaussian 09 computational package was used to perform all computations [73].

4. Conclusions

Five different Cu(II)-thiocyanato complexes were constructed from *N*-donors bidentate amine ligands including the polymeric *1D-chains* *catena*-[Cu(Me$_3$en)(μ-NCS)(NCS)] (**1**), *catena*-[Cu(NEt$_2$Meen)(μ-NCS)(NCS)] (**2**), *catena*-[Cu(N,N,2,2-Me$_4$pn)(μ-NCS)(NCS)] (**3**), the dimeric [Cu$_2$(N,N`-isp$_2$en)$_2$(μ-NCS)$_2$(NCS)$_2$] (**4**) and the monomeric complex [Cu(N,N`-*t*-Bu$_2$en)(NCS)$_2$] (**5**), where the NCS^- ions are bridging the metal centers in **1**-**4** and *N*-NCS terminal binding to the Cu^{2+} ion in **5**. The extent of nuclearity (monomer, dimer or polymer) and the thiocyanate bonding mode (N-NCS *vs.* $\mu_{N,S}$-NCS-bridging) depend entirely on the steric hindrance imposed by the *N*-alky groups introduced into the *N*-donors amines. In general, when N,N-dialkyl, N,N,N`-trialkyl- and/or tetra-N,N,N`,N`-tetraalkyl-diamines were employed as ligands, Cu(II)-(diamine)-($\mu_2$-NCS)-(*N*-NCS) 1D-polymeric chains were obtained (**1**-**3** complexes). With high sterically hindered N,N`-dialkyl bidentate amines, only Cu(II)-(diamine)(*N*-NCS)$_2$ as this was the case in compound **5**, whereas with moderate steric environment such as in N,N`-isp$_2$en, similar species to those **1**-**3** were produced but with dinuclear composition, [Cu$_2$(N,N`-isp$_2$en)$_2$(μ_2-NCS)$_2$(NCS)$_2$] (**4**).

Supplementary Material

Selected bond lengths (Å) and angles (°) for the compounds under investigation are given in Tables S1-S5 and their corresponding packing views are shown in Figures S1-S5 for **1-5** complexes, respectively.

Acknowledgements: S.S.M. acknowledges the financial support of this research by the Department of Chemistry-University of Louisiana at Lafayette. F.A.M. thanks Dr. J. Baumgartner (TU Graz) for assistance.

Author Contributions: F.A.M., R.C.F. and A.T. performed the X-ray structural analysis. S.S.M., M.M.H., A.M., H.D. and F.R.L. contributed in the synthesis and spectral characterization of the designed compounds. T.N.V.K. performed the computational study. F.A.M., S.S.M., F.R.L. and T.N.V.K. contributed to the writing of the manuscript.

Conflict of Interest: The authors declare no conflict of interest.

References

1. Shurdha, E; Moore, C.E.; Rheingold, A.L.; Lapidus, S.H.; Stephens, P.W.; Arif, A.M., Miller, J.S. *Inorg. Chem.* **2013**, 52, 10583-10594. First row transition metal(II) thiocyanate complexes, and formation of 1-, 2-, and 3-dimensional extended network structures of $M(NCS)_2(solvent)_2$ (M = Cr, Mn, Co) composition.
2. Escuera, A.; Estebana, J.; Perlepesb, S.P; Stamatatos, T.C. *Coord. Chem. Rev*. **2014**, 275, 87-129. The bridging azido as a central "player" in high-nuclearity 3d-metal cluster (M = Cr, Mn, Co) composition.
3. Palion-Gazda, J.; Machura, B.; Lloret, F.; Julve, M. *Cryst. Growth & Des.* **2015**, 15, 2380-2388. Ferromagnetic coupling through the end-to-end thiocyanate bridge in cobalt(II) and nickel(II) chains.
4. Żurowska, B.; Mroziński, J.; Julve, M.; Lloret, F.; Maslejova, A.; Sawka-Dobrowolska, W. *Inorg. Chem.* **2002**, 41, 1771–1777. Structural, spectral, and magnetic properties of end-to-end Di-μ-thiocyanato-bridged polymeric complexes of Ni(II) and Co(II). X-ray crystal structure of di-μ-thiocyanatobis(imidazole)nickel(II).
5. Rams, M.; Tomkowicz, Z.; Runecveski, T.; Böhme, M.; Plass, W.; Suckert, S.; Werner, J.; Jess, I.; Näther, *C. Phys. Chem., Chem. Phys.* **2017**, 19, 3232-3243. Influence of metal coordination and co-ligands on the magnetic properties of 1D $Co(NCS)_2$ coordination polymers.
6. Werner, J.; Tomkowic, Z.; Rams, M.; Ebbinghaus, S.G.; Neumann, T.; Näther, C. *Dalton Trans.* **2015**, 44, 14149-14158. Synthesis, structure and properties of $[Co(NCS)_2(4\text{-}(4\text{-chlorobenzyl})pyridine)_2]_n$, that shows slow magnetic relaxations and a metamagnetic transition.

7. Werner, J.; Rams, M.; Tomkowicz, Z.; Runcevski, T.; Dinnebier, R.E.; Suckert, S.; Näther, C. *Inorg. Chem.* **2015**, 54, 2893-2902. Thermodynamically metastable thiocyanato coordination polymer that shows slow relaxations of the magnetization
8. Louka, F.R.; Massoud, S.S.; Haq, T.K.; Koikawa, M.; Mikuriya, M.; Omote, M.; Fischer, R.C.; Mautner, F.A. *Polyhedron* **2017**, 138, 177-184. Synthesis, structural characterization and magnetic properties of one-dimensional Cu(II)-azido coordination polymers.
9. Massoud, S.S.; Henary, M.M.; Maxwell, L.; Martín, A.; Ruiz, E.; Vicente, R.; Fischer, R.C. Mautner, F.A. *New J. Chem.* **2018**, 42, 2627-2639. Structure, magnetic properties and DFT calculations of azido-copper(II) complexes with different azido-bonding, nuclearity and dimensionality".
10. Mautner, F.R.; Traber, M.; Fischer, R.C.; Torvisco, A.; Reichmann, K.; Speed, S.; Vicente, R.; Massoud, S.S. *Polyhedron* **2018**, 154, 436-442. Thiocyanato-4-methoxypyridine-cobalt(II) complexes with diverse geometries and a bridged 1D coordination polymer showing metamagnetic transition.
11. Massoud, S.S.; Louka, F.R.; Obaid, Y.K.; Vicente, R.; Ribas, J.; Fischer, R.C.; Mautner, F.A. *Dalton Trans.* **2013**, 42, 3968-3978. Metal ions directing the geometry and nuclearity of azido-metal(II) complexes derived from bis(2-(3,5-dimethyl-1H-pyrazol-1-yl)ethyl)-amine.
12. Mautner, F. A.; Louka, F. R.; Hofer, J.; Spell, M.; Lefèvre, A.; Guilbeau, A. E.; Massoud, S. S. *Cryst. Growth & Des.* **2013**, 13, 4518-4525. One-dimensional cadmium polymers with alternative di(EO/EE) and di(EO/EO/EO/EE) bridged azide bonding modes.
13. Świtlicka, A.; Czerwińska, K.; Machura, B.; Penkala, M.; Bieńko, A.; Bieńkod, D.; Zierkiewiczd, W. *CrystEngComm* **2016**, 18, 9042-9055. Thiocyanate copper complexes with pyrazole-derived ligands – synthesis, crystal structures, DFT calculations and magnetic properties
14. Mukherjee, S.; Mukherjee, P.S. *Acc. Chem. Res.* **2013**, 46, 2556-2566. Versatility of azide in serendipitous assembly of copper(II) magnetic polyclusters.
15. Adhikary, C., Koner, S.*Coord. Chem. Rev.* **2010**, 254, 2933-2958. Structural and magnetic studies on copper(II) azido complexes.
16. Zeng, Y.-F.; Hu, X.; Liu, F.-C.; Bu, X.-H. *Chem. Soc. Rev.* **2009**, 38, 469-480. Azido-mediated systems showing different magnetic behaviors.
17. Kettenmann, S.D.; Louka, F.R.; Marine, E.; Fischer, R.C.; Mautner, F.A.; Kulak, N.; Massoud, S.S. *Eur. J. Inorg. Chem.* **2018**, 2322-2338. Efficient artificial nucleases for mediating DNA cleavage based on tuning the steric effect in the pyridyl derivatives of tripod tetraamine-cobalt(II) complexes.
18. Massoud, S.S.; Perkins, R.S.; Louka, F.R.; Xu, W.; Le Roux, A.; Dutercq, Q.; Fischer, R.C.; Mautner, F.A.; Handa, M.; Hiraoka, Y.; Kreft, G.L.; Bortolotto, T.; Terenzi, H. *Dalton Trans.* **2014**, 43, 10086-10103. Efficient hydrolytic cleavage of plasmid DNA by chloro-cobalt(II) complexes based on sterically hindered pyridyl tripod tetraamine ligands: synthesis, crystal structure and DNA cleavage activity.
19. Massoud, S.S.; Ledet, C.C.; Junk, T.; Bosch, S.; Comba, P.; Herchel, R.; Hošek, J.; Trávníček, Z.; Fischer, R.C.; Mautner, F.A. *Dalton Trans*. **2016**, 45, 12933-1295. Dinuclear metal(II)-acetato complexes based on bicompartmental 4-chlorophenol: synthesis, structure, magnetic properties, DNA interaction and phosphodiester hydrolysis.
20. Massoud, S.S.; Louka, F.R.; Xu, W.; Perkins, R.; Vicente, R.; Albering, J.H.; Mautner, F.A. *Eur. J. Inorg. Chem.* **2011**, 3469-3479. DNA cleavage by structurally characterized dinuclear copper(II) complexes based on triazine.

21. Youngme, Y.; Phatchimkun, J.; Suksangpanya, U.; Pakawatchai, C.; van Albada, G.A.; Quesada, M.; Reedijk, J. *Inorg. Chem. Commun.* **2006**, 9, 242-247. A new unique tetranuclear Cu(II) compound with double bridging thiocyanate anions: Synthesis, X-ray structure and magnetism of $[Cu_4(\mu_{1,3}\text{-}NCS)_6(dpyam)_4(O_2CH)_2(H_2O)_2]$ (dpyam = di-2-pyridylamine).
22. Trofimenko, S.; Calabrese, J.C.; Kochi, J.K.; Wolowiec, S.; Hulsbergen, F.B.; Reedijk, J. *Inorg. Chem.* **1992,** 31, 3943-3950. Spectroscopic analysis, coordination geometry, and x-ray structures of nickel(II) compounds with sterically demanding tris(pyrazolyl)borate ligands and azide or (thio)cyanate anions. Crystal and molecular structures of bis[(μ-thiocyanato-N,S)(hydrotris(3-isopropyl-4-bromopyrazol-1-yl)borato)nickel(II)]-3-heptane and (thiocyanato-N)(hydrotris(3-tert-butyl-5-methylpyrazol-1-yl)borato)nickel(II).
23. Maity, D.; Chattopadhyay, S.; Ghosh, A.; Drew, M.G.B.; Mukhopadhyay, G. *Inorg. Chim. Acta* **2011**, 365, 25-31. Syntheses, characterization and X-ray crystal structures of a mono- and a penta-nuclear nickel(II) complex with oximato Schiff base ligands.
24. Bhowmik, P.; Chattopadhyay, S.; Drew, M.G.B.; Diaz, C.; Ghosh, A. *Polyhedron* **2010**, 29, 2637-2642. Synthesis, structure and magnetic properties of mono- and di-nuclear nickel(II) thiocyanate complexes with tridentate N3 donor Schiff bases.
25. Carranza, J.; Sletten, J.; Lloret, F.; Julve, M. *Polyhedron* **2009**, 28, 2249-1257. Preparation, crystal structures and magnetic properties of three thiocyanato-bridged copper(II) complexes with 2,2′-biimidazole or 2-(2′-pyridyl)imidazole as terminal ligands.
26. Maji, T.K.; Mostafa, G.; Clemente-Juan, J.M.; Ribas, J.; Lloret, F.; Okamoto, K.; Chaudhuri, N.R. *Eur. J. Inorg. Chem.* **2003**, 1005-1011. Synthesis, crystal structure and magneto-structural correlation of an unusual thiocyanato-bridged nickel(II) compound, $[Ni(\mu\text{-}NCS)(dpt)(NCS)]_2[Ni(\mu\text{-}NCS)(dpt)(NCS)]_4$ [dpt = bis(3-aminopropyl)amine].
27. Monfort, M.; Ribas, J.; Solans, X. *Inorg. Chem.* **1994**, 33, 4271-4276. Crystal structures and ferromagnetic properties of two new dinuclear complexes with thiocyanato bridging Ligands: $\{[Ni_2(1,2\text{-diamino-2-methylpropane})_3(NCS)_2]_2(\mu\text{-}NCS)_2\}[Ni(1,2\text{-diamino-2-methyl-propane})_2(NCS)_2]\cdot H_2O$ and $[\{Ni_2(1,2\text{-diamino-2-methylpropane})_4\}(\mu\text{-}NCS)_2](PF_6)_2$. Magneto-structural correlations.
28. Massoud, S.S.; Guilbeau, A.E.; Luong, H.T.; Vicente, R.; Albering, J.H.; Fischer, R.C.; Mautner, F.A. *Polyhedron* **2013**, 54, 26-33. Mononuclear, dinuclear and polymeric 1-D thiocyanato- and dicyanamido-copper(II) complexes based on tridentate coligands.
29. Massoud, S.S.; Mautner, F.A. *Inorg. Chim. Acta* **2005**, 358, 3334-3340. Synthesis and Structure determination of two new dinuclear end-to-end doubly bridged azido- and thiocyanato-copper(II) complexes derived from diethyldiethylenetriamine".
30. Mautner, F.A.; Louka, F.R.; Gallo, A.A.; Saber, M.R.; Burham. N.B.; Albering, J.H.; Massoud, S.S.*Transition Met. Chem.* **2010**, 35, 613-619. Thiocyanato-Cu(II) complexes derived from tridentate amine ligand and from alanine.
31. Mautner, F.A.; Vicente, R.; Massoud, S.S. *Polyhedron* **2006**, 25, 1673-1680. Structure Determination of Nitrito- and Thiocyanato-copper(II) Complexes. X-ray Structures of $[Cu(Medpt)(ONO)(H_2O)]ClO_4$ (**1**), $[Cu_2(dien)(ONO)_2]ClO_4$ (**2**) and $[Cu_2(Medpt)_2(\mu_{N,S}\text{-}NCS)_2](ClO_4)_2$ (**3**) (Medpt = 3,3`-diamino-N-methyl-dipropylamine and dien = diethylenetriamine)".
32. Wriedt, M.; Näther, C. *Eur. J. Inorg. Chem.* **2011**, 228-234. Dimorphic modifications of the thiocyanato-bridged coordination polymer $[Ni(NCS)_2(pyridazine)(H_2O)_{0.5}]_n$ with different magnetic properties.

33. You, Z.-L.; Zhu, H.-L. *Z. Anorg. Allg. Chem.* **2004**, 630, 2754-2760. Syntheses, crystal structures, and antibacterial activities of four Schiff base complexes of copper and zinc.
34. Ding, B.; Huang, Y.Q.; Liu, Y.Y.; Shi, W.; Cheng, P. *Inorg. Chem. Commun.* 2007, 10, 7-10. Synthesis, structure and magnetic properties of a novel 1D coordination polymer $\{[Cu_2(amtrz)_4(1,1\text{-}\mu\text{-}NCS)_2](ClO_4)_2\cdot H_2O\}_n$
35. Hou, L.; Li, D.; Shi, W.-J.; Yin, Y.-G.; Ng, S.W. *Inorg. Chem.* **2005**, 44, 7825-7832. Ligand-controlled mixed-valence copper rectangular grid-type coordination polymers based on pyridylterpyridine.
36. Depree, C.V. Beckmann, U.; Heslop, K.; Brooker, S. *J. Chem. Soc. Dalton Trans.* **2003**, 3071-5081. Monomeric, trimeric and polymeric assemblies of dicopper(II) complexes of a triazolate-containing Schiff-base macrocycle.
37. Hao, Z.-M.; Liu, H.-P; Han, H.-H.; Wang, W.-T.; Zhang, X.-M. *Inorg. Chem. Commun.* **2009**, 12, 375-377. A luminescent $[Ag_3S_3]_n$-tube based metal–organic framework.
38. A.O. Legendre, A.E. Mauro, J.G. Ferreira, S.R. Ananias, R.H.A. Santos, A.V.G. Netto, *Inorg. Chem. Commun.* **2007**, 10, 815-820. A 2D coordination polymer with brick-wall network topology based on the $[Cu(NCS)_2(pn)]$ monomer.
39. Lin, J.-D.; Li, Z.-H.; Li, J.-R.; Du, S.-W. *Polyhedron* **2007**, 26, 107-114. Synthesis and crystal structures of three novel coordination polymers generated from AgCN and AgSCN with flexible N-donor ligands.
40. Krautscheid, H.; Emig, N.; Klaassen, N.; Seringer, P. *J. Chem. Soc., Dalton Trans.* **1998**, 3071-3078. Thiocyanato complexes of the coinage metals: synthesis and crystal structures of the polymeric pyridine complexes $[Ag\ xCuy(SCN)_x + y(py)_z]$.
41. D. Shriver, M. Weller, T. Overtom, J, Rourke, F. Armestrong, *Inorganic Chemistry*, 6th Edn, W.H. Freeman and Company, New York, 2014, pp-139-141.
42. Mautner, F.A.; Albering, J.H.; Harrelson, E.V., Gallo, A.A.; Massoud, S.S. *J. Mol. Struct.* **2011**, 1006, 570-575. "*N*-bonding *vs. S*-bonding in Thiocyanato-copper(II) complexes.
43. Massoud, S.S.; Le Quan, L.; Gatterer, K.; Albering, J.H.; Fischer, R.C.; Mautner, F.A. *Polyhedron* **2012**, 31, 601-606. Structural characterization of five-coordinate copper(II), nickel(II), and cobalt(II) thiocyanato complexes derived from bis(2-(3,5-dimethyl-1-pyrazolyl)ethyl)amine.
44. Geary, W.J. *Coord. Chem. Rev.* **1971**, 7, 81–122. The use of conductivity measurements in organic solvents for the characterization of coordination compounds.
45. Hathaway, B.J.; Wilkinson, G.; Gillard, R.D. McCleverty, J.A. (Eds.), *Comprehensive Coordination Chemistry*, vol. 5, Pergamon, Press, Oxford, England, 1987, p. 533.
46 Näther, C.; Wöhlert, S.; Boeckmann, J.; Wriedt, M.; Jeß, I. *Z. Anorg. Allg. Chem.* **2013**, 2696-2714. A rational route to coordination polymers with condensed networks and cooperative magnetic properties.
47. Mautner, F.A., Fischer, R.C.; Rashmawi, L.G.; Louka, F.R.; Massoud, S.S. *Polyhedron* **2017**, 124, 237-242. Structural characterization of metal(II) thiocyanato complexes derived from bis(2-(1-H- pyrazol-1-yl)ethyl)amine.
48. Massoud, S.S.; Louka, F.R.; David, R.N.; Dartez, M.J.; Nguyn, Q.L.; Labry, N.J.; Fischer, R.C.; Mautner, F.A. *Polyhedron* **2015**, 90, 258-265. Five-coordinate thiocyanato- and azido-metal(II) complexes based pyrazolyl ligands.
49. Massoud, S.S.; Le Quan, L.; Gatterer, K.; Albering, J.H.; Fischer, R.C.; Mautner, F.A. *Polyhedron* **2012**, 31, 601-606. Structural Characterization of five-coordinate copper(II),

nickel(II), and cobalt(II) thiocyanato complexes derived from bis(2-(3,5-dimethyl-1-pyrazolyl)ethyl)amine.

50. Mautner, F.A.; Landry, K.N.; Gallo, A.A.; Massoud, S.S. *J. Mol. Struct.* **2007**, 837, 72-78. Molecular structure of mononuclear azido- and diacyanamido-Cu(II) complexes.
51. Shriver, E.; Weller, M.; Overton, T.; Rourke, J.; Armstrong, F. *Inorganic Chemistry*, 6th Ed, W.H. Freeman and Company, 2014, pp. 536-540.
52. Addison, A.W.; Rao, T.N.; Reedijk, J.; van Rijn, J.; Verschoor, G.C. *J. Chem. Soc., Dalton Trans.* **1984**, 1349-1356. Synthesis, structure, and spectroscopic properties of copper(II) compounds containing nitrogen-sulphur donor ligands; the crystal structure and molecular structure of aqua[1,7-bis(N-methylbenzimidazol-2'-yl)-2,6-dithiaheptane]copper(II) perchlorate,
53. Pervukhina, N.V.; Podberezskaya, N.V.; Kirichenko, N.V. *Zh. Strukt. Khim.* **1982**, *23*, 130-133. Crystal structure of isothiocyanatobis(ethylenediamine)copper(II) bromide $[Cu(en)_2(NCS)]Br$.
54. Cannas, M.; Carta, G.; Marongiu, G. *J. Chem. Soc., Dalton Trans*. **1973**, 251-254. Crystal structures of thiocyanate polyaminecopper(II) complexes. Part I. Bis(ethylenediamine)-copper(II) thiocyanate perchlorate.
55. Brown, B.W.; Lingafelter, E.C. *Acta Crystallographica* **1964**, 17, 254-259. The crystal structure of bis(ethylenediamine)copper(II) thiocyanate.
56. Koman, M.; Macaskova, L.; Ondrejovic, G.; Koren, B.; Battaglia, L.; Corradi, A. *Acta Crystallogr.* **1988**, *C44*, 245-246. Structure of bis(ethylenediamine)isothiocyanato(copper(II) tetrafluoroborate, violet isomer.
57. Garaj, J.; Dunaj-Jurco, M.; Lindgren, O. *Collect.Czech.Chem.Commun.* **1971**, 36, 3863-3873. The thiocyanate group as ligand in copper complexes the structure of the dithiocyanate ethylenediamine copper(II) complex
58. Vrábel, V.; Garaj, J.; Sivý, J.; Oktavec, D. *Acta Crystallogr*. **1999**, C55, 551-553. Aquadiisothiocyanato(N,N,N',N'-tetramethylethylenediamine-N,N')copper(II)
59. Pajunen, A.; Hamalainen, R. *Suom.Kemistil. B* **1972**, 45, 122-129. The crystal structure of bis(N-methylethylenediamine)copper(II) thiocyanate.
60. Kovenranta, J.; Pajunen, A. *Suom.Kemistil. B* **1970**, 45, 119-123. Crystal structure of bis(N,N'-dimethylethylenediamine)copper(II) thiocyanate.
61. Andreetti, G.D.; Cavalca, L.; Sgarabotto, P. *Gazz.Chim. Ital.* **1971**, 101, 483-492. Metal chelates of 1,3-diaminopropane. 1. Crystal and molecular structure of bis(1,3-diaminopropane)copper(II) thiocyanate.
62. Cannas, M.; Carta, G.; Marongiu, G. *J. Chem. Soc., Dalton Trans*. **1974**, 550-254. Crystal structures of thiocyanate polyaminecopper(II) complexes. Part II. Bis-(1,3-diaminopropane)-isothiocyanatocopper(II) perchlorate.
63. Xu, Q.; Du, M.; Song, Z.-R.; Guo, Y.-M.; Bu, X.-H. *Wuji Huaxue Xuebao(Chin.)(Chin. J. Inorg. Chem.)* **2005**, 21, 109-112. Synthesis, characterization and crystal structure of a DACO-Cu-μ-SCN complex (DACO=1,5-diazacyclooctane).
64. Wang, L.-H.; Li, L.-Z. *Acta Crystallogr.* **2007** E63, m1214-m1216. catena-Poly[[(N,N-diethylethane-1,2-diamine)thiocyanatocopper(II)]-μ-thiocyanato]
65. Espinosa, A.; Sohail, M.; Habib, M.; Naveed, K.; Saleem, M.; Rehman, H.; Hussain, I.; Munavar, A.; Ahmad, S. *Polyhedron* **2015**, 90, 252-257. Synthesis, crystal structure, theoretical calculations, and electrochemical and biological studies of polymeric (N,N,N',N'-tetramethylethylenediamine)bis(thiocyanato-κN)copper(II), $[Cu(tmeda)(NCS)_2]_n$.

66. Wang, C.-Y. *Acta Crystallogr*. **2007**, E63, m832-m834. catena-Poly[[(N,N-di-methyl-propane-1,3-di-amine)thiocyanato-copper(II)]-μ-thio-cyanato].
67. Wang, Z.-D.; Han, W.; Bian, F.; Liu, Z.-Q.; Yan, S.-P.; Liao, D.-Z.; Jiang,, Z.-H.; Cheng, P. *J. Mol. Struct*. **2005**, 733, 125-131. Synthesis, X-ray structure, spectroscopic and magnetic properties of $[Cu(DACO)(\mu\text{-}1,1\text{-}N_3)(\mu\text{-}1,3\text{-}N_3)]_n$ and $[Cu(DACO)(\mu\text{-}NCS)(NCS)]_n$ (DACO=1,5-diazacyclooctane).
68. (a) Bruker. SAINT v. 7.23; Bruker AXS Inc.: Madison, WI, USA, 2005;
(b) Bruker. APEX 2, v. 2.0-2; Bruker AXS Inc., Madison, WI, USA, 2006;
(c) Sheldrick, G.M. SADABS v. 2. University of Goettingen: Wilhelmsplatz, Germany, 2001.
69. Sheldrick, G.M. *Acta Crystallogr*. **2008**, A64, 112-122. A short history of SHELX
70. Macrae, C.F.; Edington, P.R.; McCabe, P.; Pidcock, E.; Shields, G.P.; Taylor, R.; Towler, T.; van de Streek, J. *J. Appl. Crystallogr*. **2006**, 39, 453-457. Mercury: visualization and analysis of crystal structures.
71. Kim, K.; Jordan, K.D. ". *J. Phys. Chem*. **1998**, 40, 10089–10094. Comparison of Density Functional and MP2 Calculations on the Water Monomer and Dimer.
72. Hehre, *W.J.;* Ditchfield, *R.;* Stewart, R.F.; Pople, J. A. *J. Chem. Phys*. **1970**, 52, 2769-2773. Self-consistent Molecular Orbital Methods. IV. Use of Gaussian expansions of Slater-type orbitals. Extension to second-row molecules.
73. Frisch, M.J.; Trucks, G.W.; Schlegel, H.B.; Scuseria, G.E.; Robb, M.A.; Cheeseman, J.R.; Scalmani, G.; Barone, V.; Petersson, G.A.; Nakatsuji, H.; Li, X.; Caricato, M.; Marenich, A.V.; Bloino, J.; Janesko, A.V.; Gomperts, R.; Mennucci, B.; Hratchian, H.P.; Ortiz, J.V.; Izmaylov, A.F.; Sonnenberg, J. L.; Williams-Young, D.; Ding, F.; Lipparini, F.; Egidi, Goings, J.; Peng, B.; Petrone, A.; Henderson, T.; Ranasinghe, J.; Zakrzewski, V.G.; Gao, J.; Rega, N.; Zheng, G.; Liang, W.; Hada, H.; Ehara, M.; Toyota, K.; Fukuda, R.; Hasegawa, J.; Ishida, M.; Nakajima, T.; Honda, Y.; Kitao, O.; Nakai, H.; Vreven, T.; Throssell, K.; Montgomery, J.A.; Peralta, Jr., J.E.; Ogliaro, F.; Bearpark, M.J.; Heyd, J.J.; Brothers, E.N.; Kudin, K.N.; Staroverov, V.N.; Keith, T.A.; Kobayashi, R.; Normand, J.; Raghavachari, K.; Rendell, A.B.; Burant, J.C.; Iyengar, S.S.; Tomasi, J.; Cossi, M.; Millam, J.M.; Klene, M.; Adamo, C.; Cammi, R.; Ochterski, J.W.; Martin, R.L.; Morokuma, K.; Farkas, O.; Foresman, J.B.; Fox, D.J. Gaussian, Inc., Wallingford CT, 2016.

Preprints (www.preprints.org) | NOT PEER-REVIEWED | Posted: 3 December 2018 doi:10.20944/preprints201812.0020.v1

Peer-reviewed version available at Crystals 2019, 9, 38; doi:10.3390/cryst9010038

TABLES

Table 1. The IR asymmetric stretching frequency of the coordinated thiocyanato groups and UV-Vis spectra of the complexes **1-5** in CH_3CN solution.

Complex	ν_{as}(C≡N) (cm^{-1})	λ_{max}, nm (ε, $M^{-1}cm^{-1}$)
catena-[Cu(Me$_3$en)(μ-NCS)(NCS)] (**1**)	2131 (vs), 2086 (vs)	615 (153), 974 (59)
catena-[Cu(NEt$_2$Meen)(μ-NCS)(NCS)] (**2**)	2095 (vs), 2025 (m)	655 (159)
catena-[Cu(N,N,2,2-Me$_4$pn)(μ-NCS)(NCS)] (**3**)	2099 (vs), 2068 (vs)	~656 (136)
[Cu$_2$(N,N`-isp$_2$en)$_2$(μ-NCS)$_2$(NCS)$_2$] (**4**)	2128 (s), 2073 (vs)	~655 (120)
[Cu(N,N`-*t*-Bu$_2$en)(NCS)$_2$] (**5**)	2059 (vs)	~766 (266), 469 (2160), 299 (3090)

Table 2. Some structural details of Cu(II)-thiocyanate complexes derived from some *N*-alkyl bidentate amine ligands.[a)]

Compound	C.N.; Nuc.[b)]	NCS-bonding	Refcode [Ref]
[Cu(en)$_2$]Br(NCS)	4; mono	non-coord.	BITJIX [53]
[Cu(en)$_2$](NCS)(ClO$_4$)	4; mono	non-coord.	ENCUTP [54]
[Cu(en)$_2$](NCS)$_2$	4; mono	non-coord.	EDCOPT [55]
[Cu(en)$_2$](NCS)(BF$_4$)	4; mono	non-coord.	GASRUN [56]
[Cu(en)$_2$](NCS)$_2$	4; mono	non-coord.	TCENCU [57]
[Cu(en)(NCS)$_2$(H$_2$O)]	5; mono	*N*-NCS	HIQGUJ [58]
[Cu(Me-en)$_2$(NCS)](NCS)	5; mono	*N*-NCS, non-coord.	MEENCU [59]
[Cu(N,N`-Me$_2$en)$_2$](NCS)$_2$	4; mono	non-coord.	MENCUT [60]
[Cu(propen)$_2$](NCS)$_2$	4; mono	non-coord.	APRCUT [61]
[Cu(propen)$_2$(NCS)]ClO$_4$	5; mono	*N*-NCS	DAPICU [62]
[Cu(DACO)$_2$(NCS)](NCS)(H$_2$O)	5; mono	*N*-NCS, non-coord.	FEKHAF [63]
[Cu(N,N`-*t*-Bu$_2$en)(NCS)$_2$] (**5**)	4; mono	*N*-NCS	This work
[Cu$_2$(N,N`-isp$_2$en)$_2$(μ$_2$-NCS)$_2$(NCS)$_2$] (**4**)	5, dimer	di-μ$_{N,S}$, *N*-NCS	This work
catena-[Cu(NEt$_2$en)(μ-NCS)(NCS)]	5, 1D	μ$_{N,S}$, *N*-NCS	XIBXAI [64]
catena-[Cu(Me$_4$en)(μ-NCS)(NCS)]	5; 1D	μ$_{N,S}$, *N*-NCS	DUBNIZ [65]
catena-[Cu(Me$_3$en)(μ-NCS)(NCS)] (**1**)	5, 1D	μ$_{N,S}$, *N*-NCS	This work
catena-[Cu(NEt$_2$Meen)(μ-NCS)(NCS)] (**2**)	5, 1D	μ$_{N,S}$, *N*-NCS	This work
catena-[Cu(NMe$_2$propen) (μ-NCS)(NCS)]	5; 1D	μ$_{N,S}$, *N*-NCS	SEZFAF [66]
catena-[Cu(N,N,2,2-Me$_4$pn)(μ-NCS)(NCS)] (**3**)	5, 1D	μ$_{N,S}$, *N*-NCS	This work
catena-[Cu(DACO)(μ-NCS)(NCS)]	5; 1D	μ$_{N,S}$, *N*-NCS	FODQOF [67]

[a)] Structures of the ligands and their abbreviations are shown in shown in Scheme 1.
[b)] C.N. = coordination number of Cu(II) and Nuc = nuclearity

Table 3. Crystallographic data and processing parameters for **1** – **3**.

Compound	**1**	**2**	**3**
Empirical formula	$C_7H_{14}CuN_4S_2$	$C_9H_{18}CuN_4S_2$	$C_9H_{18}CuN_4S_2$
Formula mass	281.89	309.94	309.94
System	Orthorhombic	Monoclinic	Monoclinic
Space group	$P2_12_12_1$	P $2_1/c$	P $2_1/c$
a (Å)	10.9708(6)	12.5637(13)	10.2410(11)
b (Å)	15.6954(9)	10.6338(11)	13.1290(14)
c (Å)	6.7646(4)	10.9288(12)	10.2040(11)
α (°)	90	90	90
β (°)	90	105.709(13)	92.308(19)
γ (°)	90	90	90
V (Å^3)	1164.80(12)	1405.6(3)	1370.9(3)
Z	4	4	4
T (K)	100(2)	100(2)	100(2)
μ (mm^{-1})	2.202	1.832	1.878
D_{calc} (Mg/m^3)	1.607	1.465	1.502
Crystal size (mm)	0.09 × 0.07 × 0.05	0.40 × 0.08 × 0.04	0.22 × 0.10 × 0.08
θ max (°)	33.207	26.332	25.25
Data collected	48125	10871	9720
Unique refl. / R_{int}	4443 / 0.1330	2860 / 0.0587	2469 / 0.0908
Parameters	142	151	149
Goodness-of-Fit on F^2	1.049	1.065	1.287
R1 / wR2 (all data)	0.0502 / 0.1157	0.0497 / 0.1089	0.0981 / 0.2129
Residual extrema (e/Å^3)	1.61 / -0.77	0.73 / -0.50	1.62 / -1.00

Table 4. Crystallographic data and processing parameters for **4** and **5**.

Compound	**4**	**5**
Empirical formula	$C_{20}H_{40}Cu_2N_8S_4$	$C_{12}H_{24}CuN_4S_2$
Formula mass	647.94	352.02
System	Monoclinic	Monoclinic
Space group	P $2_1/c$	P $2_1/c$
a (Å)	8.3074(10)	9.0079(11)
b (Å)	12.4648(13)	13.2386(13)
c (Å)	14.4011(15)	14.7134(14)
α (°)	90	90
β (°)	106.187(3)	103.156(3)
γ (°)	90	90
V (Å^3)	1432.1(3)	1432.1(3)
Z	2	4
T (K)	100(2)	100(2)
μ (mm^{-1})	1.802	1.516
D_{calc} (Mg/m^3)	1.503	1.368
Crystal size (mm)	0.30 × 0.18 × 0.13	0.33 × 0.22 × 0.15
θ max (°)	26.310	26.365
Data collected	11053	13358
Unique refl. / R_{int}	2894 / 0.0252	3646 / 0.0327
Parameters	164	184
Goodness-of-Fit on F^2	1.057	1.063
R1 / wR2 (all data)	0.0203 / 0.0537	0.0295 / 0.0756
Residual extrema (e/Å^3)	0.34 / -0.43	0.41 / -0.21

Preprints (www.preprints.org) | NOT PEER-REVIEWED | Posted: 3 December 2018 doi:10.20944/preprints201812.0020.v1

Peer-reviewed version available at Crystals 2019, 9, 38; doi:10.3390/cryst9010038

FIGURES

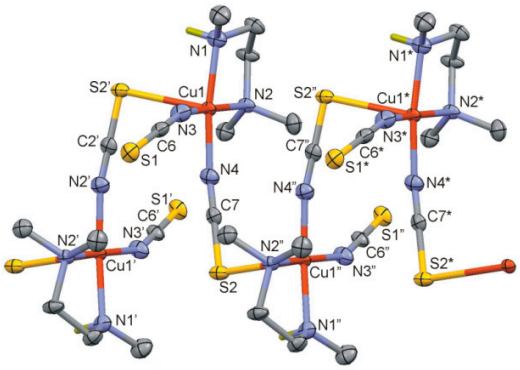

Figure 1. Perspective view of a section of the polymeric chain of **1**. Symmetry codes: (‘) 3/2-x,1-y,1/2+z; (“) 3/2-x,1-y,-1/2+z; (*) x,y,-1+z.

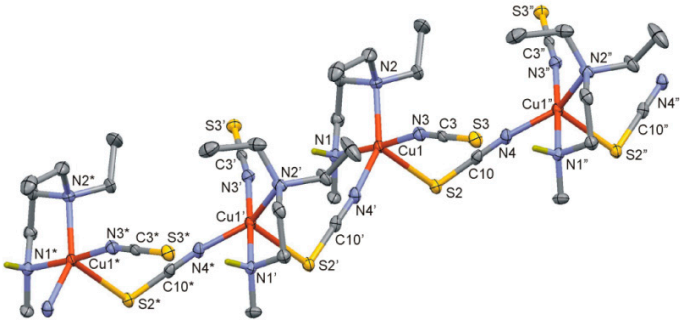

Figure 2. Perspective view of a section of the polymeric chain of **2**. Symmetry codes: (‘) x,1/2-y,-1/2+z; (“) x,1/2-y,1/2+z; (*) x,y,-1+z.

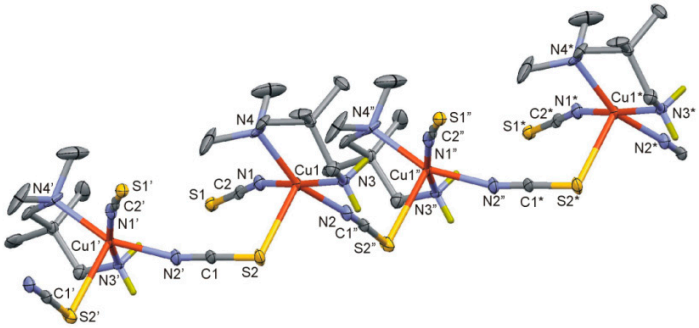

Figure 3. Perspective view of a section of the polymeric chain of **3**. Symmetry codes: (‘) x,1/2-y,1/2+z; (“) x,1/2-y,-1/2+z; (*) x,y,-1+z.

Preprints (www.preprints.org) | NOT PEER-REVIEWED | Posted: 3 December 2018 doi:10.20944/preprints201812.0020.v1

Peer-reviewed version available at Crystals 2019, 9, 38; doi:10.3390/cryst9010038

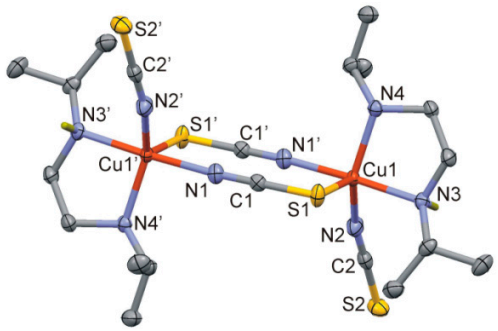

Figure 4. Perspective view of the dimeric complex **4**. Symmetry code: (') 2-x,-y,-z.

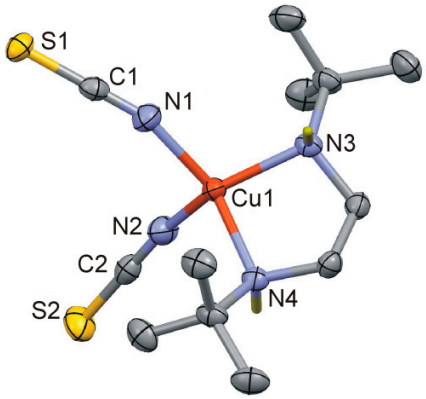

Figure 5. Molecular plot of **5**.

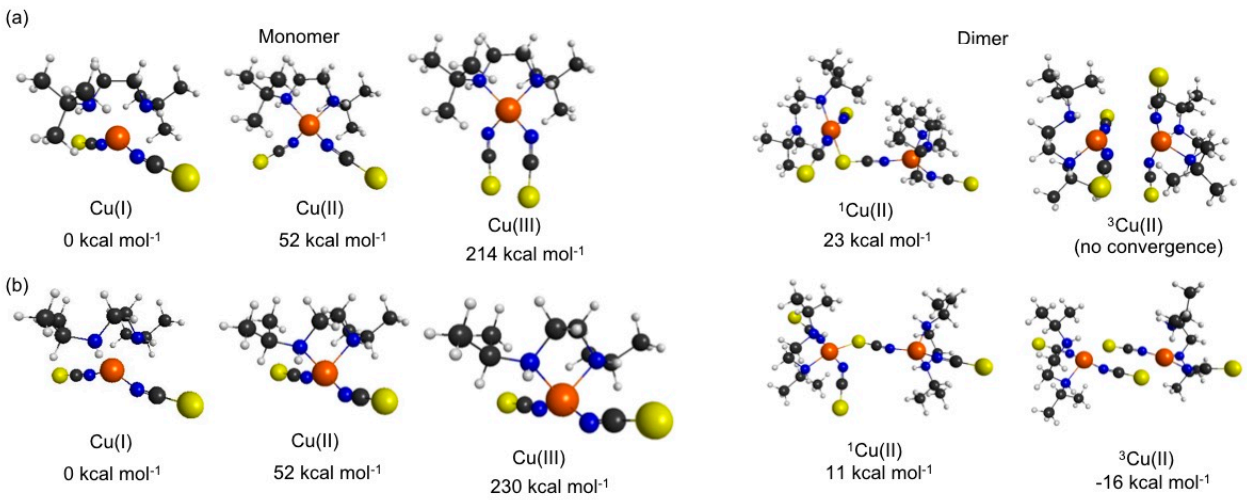

Figure 6. Geometries associated with the ground state minima of (a) 5 and (b) 4. The Dimer geometries are relative to the energy of the Cu(II) + Cu(II) monomer asymptote at infinite separation.

SUPPLEMENTARY MATERIALS

Steric Effects of Alkyl Substituents at *N*-Donor Bidentate Amines Directs the Nuclearity, Bonding and Bridging Modes in Thiocyanato-Copper(II) Complexes

Franz A. Mautner [1,*], Roland C. Fischer [2], Ana Torvisco [2], Maher M. Henary [3], Andrew Milner [4], Hunter DeVillier [4], Tolga N. V. Karsili [4], Febee R. Louka [4] and Salah S. Massoud [4,*]

[1] Institut für Physikalische and Theoretische Chemie, Technische Universität Graz, A-8010 Graz, Austria; mautner@tugraz.at

[2] Institut für Anorganische Chemie, Technische Universität Graz, Stremayrgasse 9/V, A-8010 Graz, Austria; roland.fischer@tugraz.at, ana.torviscogomez@tugraz.at

[3] Department of Chemistry and Biochemistry, University of California, Los Angeles, CA 90095-1569, U.S.A. henary@chem.ucla.edu

[4] Department of Chemistry, University of Louisiana at Lafayette, P.O. Box 43700 Lafayette, LA 70504, U.S.A. tolga.karsili@louisiana.edu (T.K.); frl6631@louisiana.edu (F.R.L.); ssmassoud@louisiana.edu (S.S.M.); C00250551@louisiana.edu (A.M.); C00063128@louisiana.edu (H.De.V)

Table of Contents

Table S1. Selected bond lengths (Å) and angles (°) for compound **1**.

Table S2. Selected bond lengths (Å) and angles (°) for compound **2**.

Table S3. Selected bond lengths (Å) and angles (°) for compound **3**.

Table S4. Selected bond lengths (Å) and angles (°) for compound **4**.

Table S5. Selected bond lengths (Å) and angles (°) for compound **5**.

Figure S1: Packing plot of compound **1**.

Figure S2: Packing plot of compound **2**.

Figure S3: Packing plot of compound **3**.

Figure S4: Packing plot of compound **4**.

Figure S5: Packing plot of compound **5**.

Preprints (www.preprints.org) | NOT PEER-REVIEWED | Posted: 3 December 2018 doi:10.20944/preprints201812.0020.v1

Peer-reviewed version available at Crystals 2019, 9, 38; doi:10.3390/cryst9010038

Table S1. Selected bond lengths (Å) and angles (°) for compound **1**.

Cu(1)-N(4)	1.952(4)	Cu(1)-N(3)	1.966(4)
Cu(1)-N(1)	2.024(4)	Cu(1)-N(2)	2.066(3)
C(6)-N(3)	1.167(6)	C(6)-S(1)	1.633(4)
C(7)-N(4)	1.150(6)	C(7)-S(2)	1.640(4)
Cu(1)-S(2')	2.8910(16)		
N(4)-Cu(1)-N(3)	89.43(16)	N(4)-Cu(1)-N(1)	172.27(19)
N(3)-Cu(1)-N(1)	93.99(16)	N(4)-Cu(1)-N(2)	90.02(14)
N(3)-Cu(1)-N(2)	171.9(2)	N(1)-Cu(1)-N(2)	85.62(14)
N(3)-C(6)-S(1)	178.6(5)	N(4)-C(7)-S(2)	179.4(4)

Symmetry code: (‘): 3/2-x,1-y,1/2+z.

Table S2. Selected bond lengths (Å) and angles (°) for compound **2**.

Cu(1)-N(3)	1.957(3)	Cu(1)-N(4')	1.992(3)
Cu(1)-N(1)	2.009(3)	Cu(1)-N(2)	2.094(3)
Cu(1)-S(2)	2. 6421(11)	S(2)-C(10)	1.642(4)
S(3)-C(3)	1.637(4)	N(3)-C(3)	1.166(5)
C(10)-N(4')	1.152(5)		
N(3)-Cu(1)-N(4')	92.93(13)	N(3)-Cu(1)-N(1)	175.57(13)
N(4)-Cu(1)-N(1)	88.29(13)	N(3)-Cu(1)-N(2)	92.16(13)
N(4)-Cu(1)-N(2)	150.30(12)	N(1)-Cu(1)-N(2)	84.70(12)
N(3)-Cu(1)-S(2)	93.29(9)	N(4)-Cu(1)-S(2)	99.49(9)
N(1)-Cu(1)-S(2)	90.70(10)	N(2)-Cu(1)-S(2)	109.40(9)
C(10)-S(2)-Cu(1)	98.70(13)	C(3)-N(3)-Cu(1)	164.1(3)
N(3)-C(3)-S(3)	178.8(3)	N(4')-C(10)-S(2)	179.8(4)
C(10')-N(4')-Cu(1)	167.7(3)		

Symmetry code: (‘): x,1/2-y,-1/2+z.

Table S3. Selected bond lengths (Å) and angles (°) for compound **3**.

Cu(1)-N(1)	1.959(8)	Cu(1)-N(3)	1.978(7)
Cu(1)-N(2)	2.022(7)	Cu(1)-N(4)	2.106(7)
Cu(1)-S(2)	2.618(2)	S(1)-C(2)	1.635(10)
S(2)-C(1)	1.640(9)	N(1)-C(2)	1.167(12)
N(2')-C(1)	1.167(11)		
N(1)-Cu(1)-N(3)	169.7(3)	N(1)-Cu(1)-N(2)	87.0(3)
N(3)-Cu(1)-N(2)	85.8(3)	N(1)-Cu(1)-N(4)	90.9(3)
N(3)-Cu(1)-N(4)	92.9(3)	N(2)-Cu(1)-N(4)	157.4(3)
N(1)-Cu(1)-S(2)	95.9(2)	N(3)-Cu(1)-S(2)	92.7(2)
N(2)-Cu(1)-S(2)	100.3(2)	N(4)-Cu(1)-S(2)	102.2(2)
C(3)-S(2)-Cu(1)	99.3(3)	C(2)-N(1)-Cu(1)	164.7(7)
C(1")-N(2)-Cu(1)	155.8(8)		

Symmetry codes: (‘): x,-1/2-y,z+1/2; (“): x,1/2-y,z-1/2.

Table S4. Selected bond lengths (Å) and angles (°) for compound **4**.

Cu(1)-N(1)	1.9487(13)	Cu(1)-N(2)	1.9714(12)
Cu(1)-N(3)	2.0314(12)	Cu(1)-N(4)	2.0388(12)
N(1)-C(1)	1.1562(19)	C(1)-S(1)	1.6420(14)
N(2)-C(2)	1.1612(19)	C(2)-S(2)	1.6306(19)
N(1)-Cu(1)-N(2)	92.77(5)	N(1)-Cu(1)-N(3)	173.69(5)
N(2)-Cu(1)-N(3)	90.06(5)	N(1)-Cu(1)-N(4)	95.60(5)
N(2)-Cu(1)-N(4)	143.81(5)	N(3)-Cu(1)-N(4)	85.38(5)
C(1)-N(1)-Cu(1)	173.82(11)	N(1)-C(1)-S(1)	179.19(13)
C(3)-N(2)-Cu(1)	163.99(11)	N(2)-C(2)-S(2)	178.89(13)

Table S5. Selected bond lengths (Å) and angles (°) for compound **5**.

Cu(1)-N(1)	1.9380(17)	Cu(1)-N(3)	2.0108(16)
Cu(1)-N(2)	1.9299(17)	Cu(1)-N(2)	2.0043(15)
C(1)-N(1)	1.156(3)	C(1)-S(1)	1.637(2)
C(2)-N(2)	1.165(3)	C(2)-S(2)	1.618(2)
N(1)-Cu(1)-N(2)	97.93(7)	N(2)-Cu(1)-N(4)	97.03(7)
N(1)-Cu(1)-N(4)	140.14(7)	N(2)-Cu(1)-N(3)	138.36(7)
N(1)-Cu(1)-N(3)	104.87(7)	N(3)-Cu(1)-N(4)	87.35(6)
Cu(1)-N(1)-C(1)	161.74(16)	Cu(1)-N(2)-C(2)	160.42(17)
N(1)-C(1)-S(1)	179.08(18)	N(2)-C(2)-S(2)	179.6(2)

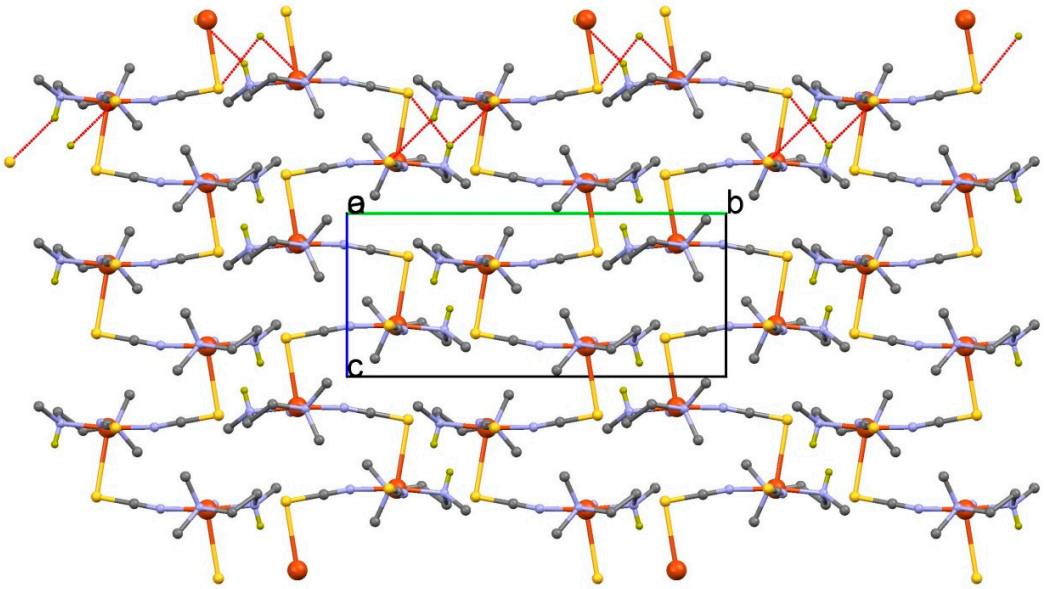

Figure S1. Packing plot of compound **1**.

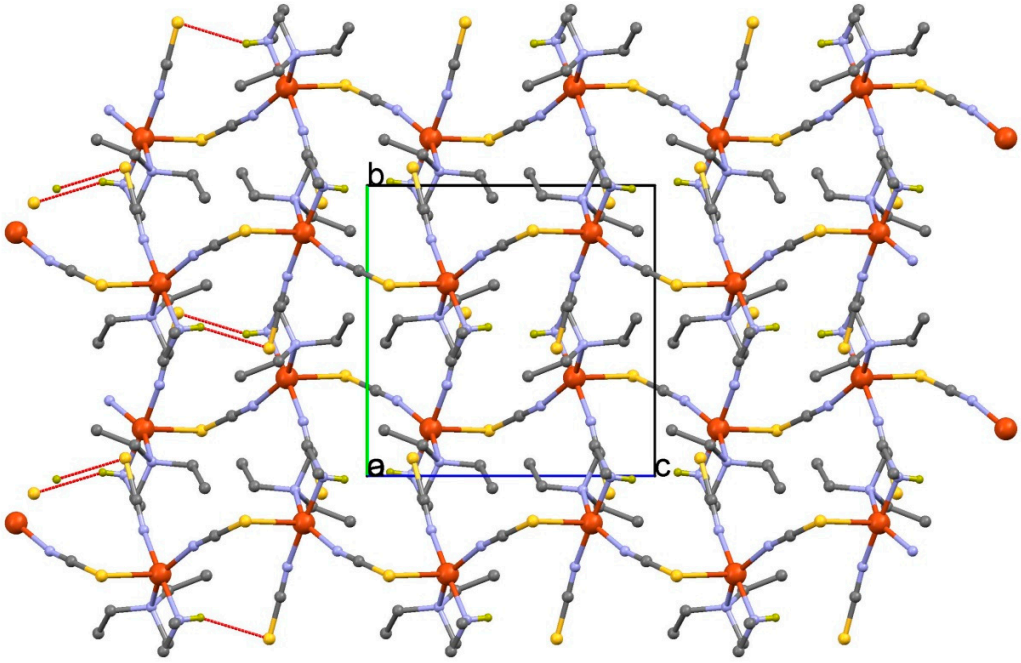

Figure S2. Packing plot of compound **2**.

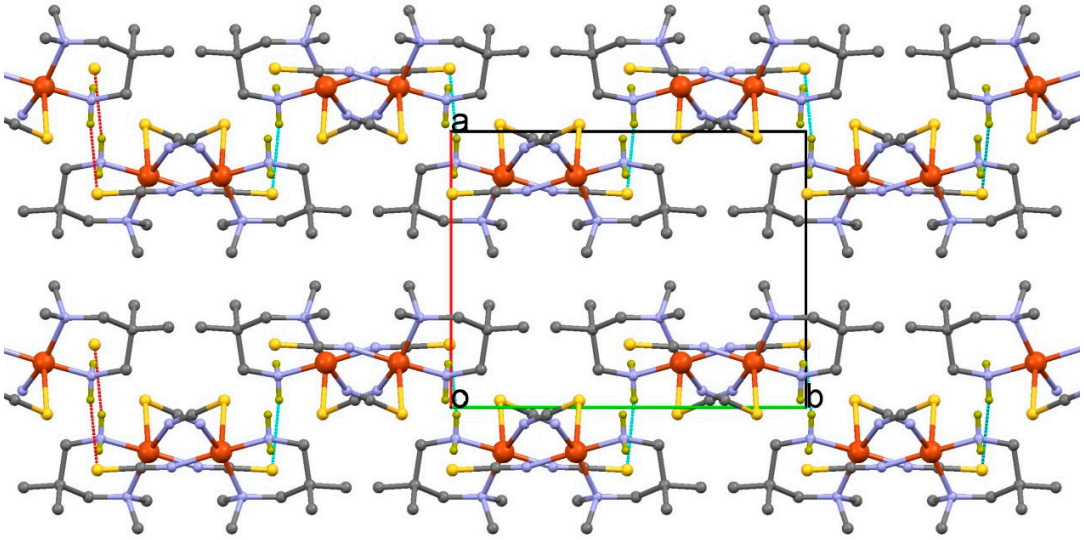

Figure S3. Packing plot of compound **3**.

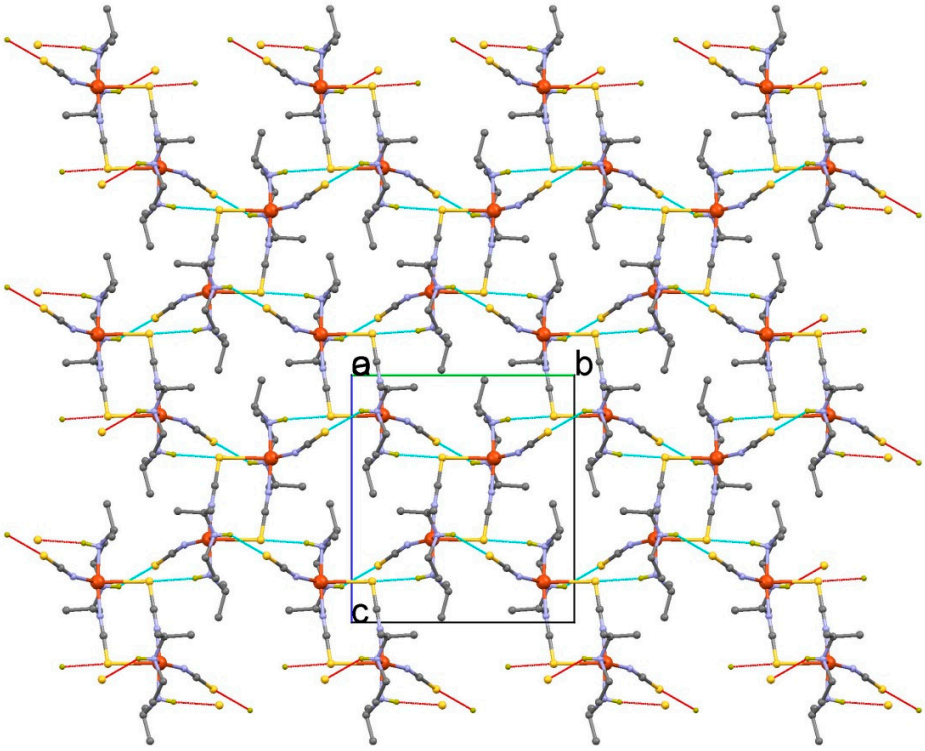

Figure S4. Packing plot of compound **4**.

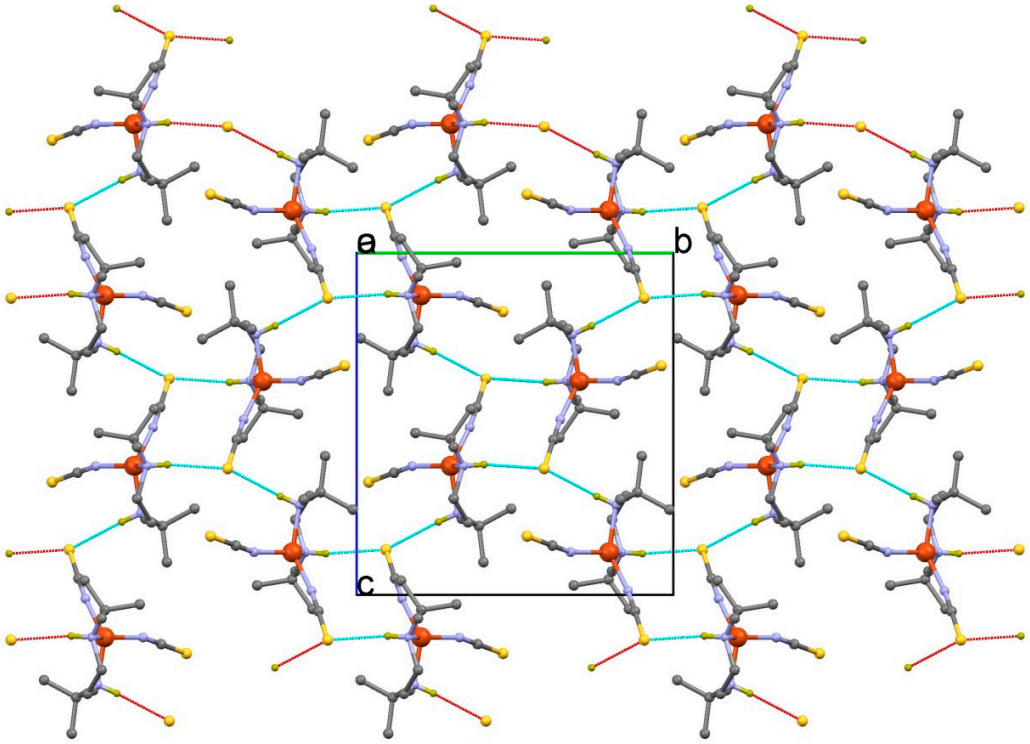

Figure S5. Packing plot of compound **5**.